grant-in-aid for Research on Publicly Essential Drugs and Medical Devices from the Japan Health Science Foundation, and a grant-in-aid from the Ministry of Health, Labour, and Welfare of Japan.

References

1 Khorasanizadeh S, Rastinejad F. Nuclear-receptor interactions on DNA-response elements. Trends Biochem Sci. 2001;26:384–390.

2 Makishima M, Okamoto AY, Repa JJ, Tu H, Learned RM, Luk A, et al. Identification of a nuclear receptor for bile acids. Science. 1999;284:1362–1365.

3 Parks DJ, Blanchard SG, Bledsoe RK, Chandra G, Consler TG, Kliewer SA, et al. Bile acids: natural ligands for an orphan nuclear receptor. Science. 1999;284:1365–1368.

4 Wang H, Chen J, Hollister K, Sowers LC, Forman BM. Endogenous bile acids are ligands for the nuclear receptor FXR/BAR. Mol Cell. 1999;3:543–553.

5 Sinal CJ, Tohkin M, Miyata M, Ward JM, Lambert G, Gonzalez FJ. Targeted disruption of the nuclear receptor FXR/BAR impairs bile acid and lipid homeostasis. Cell. 2000;102:731–744.

6 Maloney PR, Parks DJ, Haffner CD, Fivush AM, Chandra G, Plunket KD, et al. Identification of a chemical tool for the orphan nuclear receptor FXR. J Med Chem. 2000;43:2971–2974.

7 Liu Y, Binz J, Numerick MJ, Dennis S, Luo G, Desai B, et al. Hepatoprotection by the farnesoid X receptor agonist GW4064 in rat models of intra- and extrahepatic cholestasis. J Clin Invest. 2003;112:1678–1687.

8 Zhang Y, Lee FY, Barrera G, Lee H, Vales C, Gonzalez FJ, et al. Action of the nuclear receptor FXR improves hyperglycemia and hyperlipidemia in diabetic mice. Proc Natl Acad Sci U S A. 2006;103:1006–1011.

9 Inagaki T, Moschetta A, Lee Y-K, Peng L, Zhao G, Downes M, et al. Regulation of antibacterial defense in the small intestine by the nuclear bile acid receptor. Proc Natl Acad Sci U S A. 2006;103:3920–3925.

10 Cui J, Huang L, Zhao A, Lew J-L, Yu J, Sahoo S, et al. Guggulsterone is a farnesoid X receptor antagonist in coactivator association assays but acts to enhance transcription of bile salt export pump. J Biol Chem. 2003;278:10214–10220.

11 Dussault I, Beard R, Lin M, Hollister K, Chen J, Xiao JH, et al. Identification of gene-selective modulators of the bile acid receptor FXR. J Biol Chem. 2003;278:7027–7033.

12 Suzuki T, Nishimaki-Mogami T, Kawai H, Kobayashi T, Shinozaki Y, Sato Y, et al. Screening of novel nuclear receptor agonists by a convenient reporter gene assay system using green fluorescent protein derivatives. Phytomedicine. 2006;13:401–411.

13 Asakawa Y. Chemical constituents of hepaticae. In: Herz W, Grisebach H, Kirby WG, editors. Progress in the chemistry of organic natural products, Vol. 42, Wien: Spriger; 1982, p. 1–285.

14 Asakawa Y. Biologically active terpenoids and aromatic compounds from liverworts and inedible mushroom *Cryptoporus volvatus*. In: Colegate SM, Molyneux RJ, editors. Bioactive natural products: detection, isolation, and structural determination. Florida: CRC Press; 1993, p. 319–347.

15 Mi L-Z, Devarakonda S, Harp JM, Han Q, Pellicciari R, Willson TM, et al. Structural basis for bile acid binding and activation of the nuclear receptor FXR. Mol Cell. 2003;11:1093–1100.

16 Lew JL, Zhao A, Yu J, De Pedro N, Peláez F, Wright SD, et al. The farnesoid X receptor controls gene expression in a ligand- and promoter-selective fashion. J Biol Chem. 2004;279:8856–8861.

17 Gupta S, Stravitz RT, Dent P, Hylemon PB. Down-regulation of cholesterol 7α-hydroxylase (*CYP7A1*) gene expression by bile acids in primary rat hepatocytes is mediated by the c-Jun N-terminal kinase pathway. J Biol Chem. 2001;276:15816–15822.

18 Staudinger JL, Goodwin B, Jones SA, Hawkins-Brown D, MacKenzie KI, LaTour A, et al. The nuclear receptor PXR is a lithocholic acid sensor that protects against liver toxicity. Proc Natl Acad Sci U S A. 2001;98:3369–3374.

19 Asakawa Y. Recent advances in phytochemistry of bryophytes-acetogenins, terpenoids and bis(bibenzyl)s from selected Japanese, Taiwanese, New Zealand, Argentinean and European liverworts. Phytochemistry. 2001;56:297–312.

20 Qiao L, Han SI, Fang Y, Park JS, Gupta S, Gilfor D, et al. Bile acid regulation of C/EBPβ, CREB, and c-Jun function, via the extracellular signal-regulated kinase and c-Jun NH_2-terminal kinase pathways, modulates the apoptotic response of hepatocytes. Mol Cell Biol. 2003;23:3052–3066.

21 Fischer S, Beuers U, Spengler U, Zwiebel FM, Koebe HG. Hepatic levels of bile acids in end-stage chronic cholestatic liver disease. Clin Chim Acta. 1996;251:173–186.

22 Javitt NB. Cholestasis in rats induced by taurolithocholate. Nature. 1966;210:1262–1263.

23 Kodera Y, Takeyama K, Murayama A, Suzuwa M, Masuhiro Y, Kato S. Ligand type-specific interactions of peroxisome proliferator-activated receptor gamma with transcriptional coactivators. J Biol Chem. 2000;275:33201–33204.

24 Shang Y, Brown M. Molecular determinants for the tissue specificity of SERMs. Science. 2002;295:2465–2468.

25 Modica S, Moschetta A. Nuclear bile acid receptor FXR as pharmacological target: are we there yet? FEBS Lett. 2006;580:5492–5499.

26 Cariou B, Staels B. FXR: A promising target for the metabolic syndrome? Trends Pharmacol Sci. 2007;28:236–243.

J. Biochem. 143, 537–545 (2008)
doi:10.1093/jb/mvm248

Annexin A3 Expression Increases in Hepatocytes and is Regulated by Hepatocyte Growth Factor in Rat Liver Regeneration

Mizuho Harashima[1], Kayo Harada[1], Yoshimasa Ito[1], Masashi Hyuga[2], Taiichiro Seki[1], Toyohiko Ariga[1], Teruhide Yamaguchi[2] and Shingo Niimi[2,*]

[1]Department of Nutrition and Physiology, Nihon University College of Bioresource Sciences, Kameino Fujisawa 252-8510; and [2]Division of Biological Chemistry and Biologicals, National Institute of Health Sciences, 1-18-1 Kamiyoga, Setagaya-ku, Tokyo 158-8501, Japan

Received November 14, 2007; accepted December 18, 2007; published online January 7, 2008

Annexin (Anx) A3 increases and plays important roles in the signalling cascade in hepatocyte growth in cultured hepatocytes. However, no information is available on its expression and role in rat liver regeneration. In the present study, AnxA3 expression was investigated to determine whether it also plays a role in the signalling cascade in rat liver regeneration. AnxA3 protein and mRNA level both increase in liver after administration of carbon tetrachloride (CCl_4) or 70% partial hepatectomy. AnxA3 protein level increases in isolated parenchymal hepatocytes, but not in non-parenchymal liver cells, in these rat liver regeneration models. AnxA3 mRNA increases in hepatocytes after CCl_4 administration. Anti-hepatocyte growth factor antibody suppresses this increase in AnxA3 mRNA level. These results demonstrate that AnxA3 expression increases in hepatocytes through a hepatocyte growth factor-mediated pathway in rat liver regeneration models, suggesting that AnxA3 plays an important role in the signalling cascade in rat liver regeneration.

Key words: annexin A3, carbon tetrachloride, hepatocyte growth factor, parenchymal hepatocytes, partial hepatectomy.

Abbreviations: Anx, Annexin; CCl_4, carbon tetrachloride; HGF, hepatocyte growth factor.

Annexin (Anx) A3 is a member of the Anx family, which binds to phospholipids and membranes in a Ca^{2+}-dependent manner (*1–4*). AnxA3 has been shown to have anti-coagulant and anti-phospholipase A_2 properties *in vitro* (*5*, *6*), plus to promote Ca^{2+}-dependent aggregation of isolated specific granules from human neutrophils (*5*, *6*). Some reports describe its regulation and role in cultured cells (*7–11*); however, there are no reports describing these characteristics *in vivo*.

We recently reported that AnxA3 is expressed in cultured rat hepatocytes, but not in isolated hepatocytes and that inhibition of AnxA3 expression by RNA interference results in a significant inhibition of hepatocyte growth (*10*, *12*, *13*). These findings indicate that AnxA3 plays an important role in the signalling cascade in hepatocyte growth in cultured hepatocytes, although the mechanism remains to be elucidated. The significance of AnxA3 in hepatocyte growth is also supported by the finding that known stimulatory or inhibitory actions of various factors to hepatocyte growth correlated well with the increase or decrease in AnxA3 expression (*14*).

These findings indicate that AnxA3 increases and is likely to play an important role in the signalling cascade in rat liver regeneration. AnxA1 increases in rat and mouse liver regeneration models, *e.g.* after administration of carbon tetracholoride (CCl_4) and 70% partial hepatectomy (*15*, *16*). Suppression of AnxA1 expression using anti-sense technology inhibits proliferation in a mouse hepatocyte cell line (*15*). Therefore, AnxA1 is also likely to play an important role in the signalling cascade in rat liver regeneration.

In the present study, AnxA3 expression in rat liver regeneration models was investigated to explore the possibility that AnxA3 plays important roles in the signalling cascade in rat liver regeneration.

MATERIALS AND METHODS

Animals and Experimental Conditions—Adult male Wistar rats (180–200 g) were purchased from Japan SLC Co., Ltd. (Shizuoka, Japan) and used for all studies. They were maintained in a 12 h light/dark cycle, allowed food and water *ad libitium*. All animal care and procedures were approved by the institutional care committee and carried out in accordance with the guidelines established by the National Institute of Health.

For studies of liver regeneration after toxic injury, rats received CCl_4 intraperitoneally (2 ml/kg body weight of 50% solution of CCl_4 in olive oil). Control rats received olive oil intraperitoneally (1 ml/kg body weight of olive oil). Animals given CCl_4 or olive oil were sacrificed at 3–24 h after administration.

A 70% partial hepatectomy was performed according to Higgins and Anderson (*17*). In the sham operation, livers were exposed and manipulated but not removed. These procedures were performed under anaesthesia with Nembutal (Abbot, Chicago, IL, USA). Animals subjected to

*To whom correspondence should be addressed. Tel: +81-3-3700-9347, Fax: +81-3-3700-9084, E-mail: niimi@nihs.go.jp

partial hepatectomy or sham operation were sacrificed at 2.5–20 h after the operation.

For infusion of anti-human hepatocyte growth factor (HGF) antibody, rats were intravenously injected with 0.2 ml goat anti-human HGF IgG (Sigma–Aldrich, St Louis, MO, USA) (1.25 mg/kg body weight) diluted in phosphate-buffered saline (PBS) through the tail vein, then received CCl_4 intraperitoneally, as described earlier. Control rats were injected with the same volume and amount of control goat IgG, and then received CCl_4 intraperitoneally in a similar manner. Parenchymal hepatocytes were prepared from the rats after 6 h, as described subsequently.

Preparation of Liver Lysate—The procedures were performed at low temperature, unless described otherwise. Liver was *in situ* perfused with PBS *via* the portal vein, then removed from the body. Liver was homogenized with a Potter-Elvehjem homogenizer in 4× (v/w) buffer A [50 mM Tris–HCl (pH 7.5), 150 mM NaCl, 10 mM EDTA and 2.5% (v/v) Triton-X 100] containing 1 mM benzylsulphonyl fluoride, 0.3 mM leupeptin and 0.5 mM aprotinin. The homogenate was shaken for 15 min at room temperature, then sonicated four times for 15 s each time. After centrifugation at 100,000*g*, the cytosolic fraction was stored at −70°C until use.

Cell Isolation—Parenchymal hepatocytes were isolated from rats by *in situ* perfusion of the liver with collagenase (*18*). Non-parenchymal liver cells were isolated from the supernatant of parenchymal cells by differential centrifugation, as described by Shimaoka *et al.* (*19*). In this article, hepatocytes are also referred to as parenchymal hepatocytes to distinguish between hepatocytes and non-parenchymal liver cells.

Preparation of Cell Lysate—Cell lysates were prepared by a modification of the reported by Römisch *et al.* (*20*). Procedures were performed at low temperature, unless described otherwise. Cells were resuspended in three volumes of buffer A containing 1/100 (v/v) protease inhibitor cocktail (Sigma–Aldrich, St Louis, MO, USA). They were then shaken for 15 min at room temperature and sonicated four times for 15 s each time. After centrifugation at 100,000*g*, the cytosolic fraction was stored at −70°C until use.

Western Blot Analysis—An equal amount of cytosolic protein from each experiment was subjected to SDS–PAGE on a 10% gel and electroblotted to PVDF membrane (GVHP; Millipore, Bedford, MA, USA). After blocking the membrane with 5% skimmed milk, a western blot analysis was performed using rabbit anti-human AnxA3 antibody serum (1: 5,250) (a gift from Drs F. Russo-Marie and C. Ragueness-Nicol), mouse anti-human GAPDH monoclonal antibody (1: 5,000) (Abcam, Cambridge, UK), or rabbit anti-beta-actin polyclonal antibody (1: 500) (BioLegend, San Diego, CA, USA). Detection was performed using the ECL detection system (GE Health care Bioscience, Buckinghamshire, UK). Housekeeping protein, GAPDH and beta-actin, were selected based on results of preliminary studies. Intensity of each band was measured over a proportional range. A computer-assisted analyser was used to quantitatively analyse intensity, with intensity of the AnxA3 band normalized to the intensity of the appropriate housekeeping protein. Protein amount from liver and cell lysate was measured using a previously described method (*21*), with bovine serum albumin used as a standard.

Total RNA Extraction and Real-Time Quantitative PCR—Total RNA was extracted from liver by a modification of guanidine thiocyanate–phenol–chloroform extraction method (*22*, *23*). Total RNA was extracted from cells using Trizol® reagent (Invitrogen, Cergy Pontoise, France) in accordance with the manufacture's protocol. Equal amounts of RNA (~1 μg) from each experiments were reverse-transcribed using a THERMOSCRIPT™ RT–PCR System (Invitrogen, Cergy Pontoise, France) and oligo$(dT)_{20}$ in a final volume of 40 μl, in accordance with the manufacturer's protocol. Subsequently, 2 μl of cDNA was used as templates for real-time PCR analysis using a LightCycler system (Rosche Diagnostics, Tokyo, Japan) according to the manufacture's instructions. For AnxA3 and 28S rRNA, the PCR programme consisted of 40 cycles of 10 s at 94°C, 10 s at 60°C and 12 s at 72°C. Primer sequences for AnxA3 were 5′ -CAA ATT CAC CGA GAT CCT GT-3′ and 5′ -TGC TGG AGT GCT GTA CGA AA-3′ (*14*) and for 28S rRNA 5′ -CCA GAG CGA AAG CAT TTG CCA-3′ and 5′ -GGC ATC ACA GAC CTG TTA TTG CTC-3′ (*14*). AnxA3 levels were normalized to the levels of 28S rRNA.

Statistical Analysis—Data were analysed using Student's *t*-test, and *P*-values <0.05 were considered to be statistically significant.

Immunohistochemical Examination—Serial liver sections cut at 3 μm thick from the paraformaldehyde-fixed and paraffin-embedded blocks. De-paraffinated and re-hydrated sections were heated for 5 min at 100°C in 10 mM citrate buffer (pH 6.0) followed by the treatment with 10 μg/ml Proteinase K (TAKARA BIO Inc., Shiga, Japan) for 5 min at room temperature. These activated sections were then subjected to blocking with 10% bovine serum albumin for 1 h at room temperature. After washing with PBS, sections were simultaneously incubated for 2 h with antibodies, *e.g.* anti-rat hepatic sinusoidal endothelial cells mouse IgG (SE-1, Immuno-Biological Laboratories Co., Ltd. Gunma, Japan) 1:20 and rabbit anti-human AnxA3 antibody serum 1:200. The fluorescence-labelled secondary antibodies were AMCA-labelled sheep anti-mouse IgG (Jackson Immuno Research Laboratories, Inc., PA, USA) 1:200 and FITC-labelled sheep anti-rabbit IgG (MP Biomedicals Inc., Ohio, USA) 1:200. The liver sections were thus mounted on a cover glass with a mounting medium, Vectashield (Vector Laboratories, CA, USA), and subjected to microscopic observation.

RESULTS

AnxA3 Expression in Liver Following CCl_4 Treatment—AnxA3 protein level increased ~3-fold at 6 h after administration of CCl_4 and this increased level was maintained to 24 h (Fig. 1). AnxA3 mRNA level started to increase at 3 h after administration, reaching an ~17-fold increase at 24 h (Fig. 2).

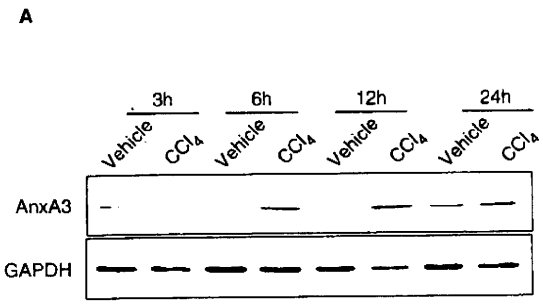

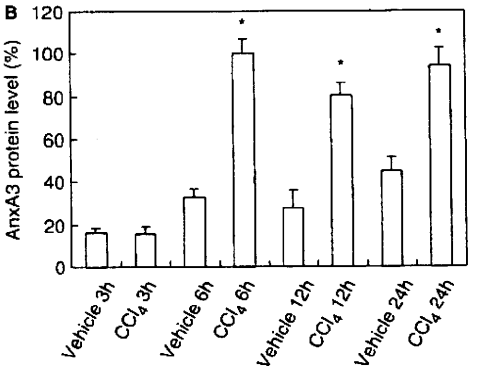

Fig. 1. **AnxA3 protein level in liver following treatment with CCl_4.** (A) Data shown are representative of western blot analysis results. Approximately 35 and 1.5 μg of protein were used for detection of AnxA3 and GAPDH, respectively. (B) Results are presented relative to the value produced by liver in rats at 6 h after CCl_4 administration. AnxA3 protein levels were normalized to the housekeeping protein, GAPDH. Data are expressed as mean ± S.D. ($n = 4$ at each time point) $^*P < 0.01$, compared to the value produced by liver in rats after olive oil administration.

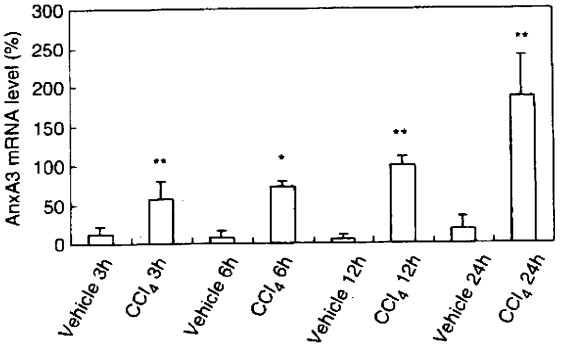

Fig. 2. **AnxA3 mRNA level in liver following treatment with CCl_4.** Results are presented relative to the value produced by liver in rats at 6 h after CCl_4 administration ($n = 4$ at each time point). AnxA3 mRNA levels were normalized to housekeeping gene, 28S rRNA. Data are expressed as the mean ± SD ($n = 4$ at each time point) $^*P < 0.01$, $^{**}P < 0.05$, compared to the value produced by liver in rats after olive oil administration.

AnxA3 Expression in Parenchymal Hepatocytes and Non-parenchymal Liver Cells Following CCl_4 Treatment—Parenchymal hepatocytes and/or non-parenchymal liver cells are involved in the increase of AnxA3 expression in liver following CCl_4 treatment. AnxA3 protein level increased ~5-fold in parenchymal hepatocytes at 6 h after CCl_4 treatment, but did not change in non-parenchymal liver cells (Fig. 3). AnxA3 mRNA level increased ~5-fold in parenchymal hepatocytes at 6 h after CCl_4 treatment; however, it did not change in non-parenchymal liver cells (Fig. 4).

AnxA3 Expression in Liver after Partial Hepatectomy—AnxA3 protein level started to increase at 5 h after partial hepatectomy, reaching a 1.6-fold increase at 20 h (Fig. 5). AnxA3 mRNA level increased to ~2,800-fold at 2.5 h, then began decreasing at 5 h, falling back to basal level at 20 h (Fig. 6).

AnxA3 Expression in Parenchymal Hepatocytes and Non-parenchymal Liver Cells After Partial Hepatectomy—AnxA3 protein level increased ~1.5-fold in isolated parenchymal hepatocytes at 6 h after partial hepatectomy, but did not change in non-parenchymal liver cells (Fig. 7). AnxA3 mRNA level decreased to ~80% in hepatocytes at 6 h after partial hepatectomy; however, AnxA3 mRNA did not change in non-parenchymal liver cells (Fig. 8).

AnxA3 Expression in Hepatic Sinusoidal Endothelial Cells—Non-parenchymal liver cells expressing AnxA3 were investigated by immunohistochemical staining. Hepatic sinusoidal endothelial cells were chosen as a candidate, as human umbilical vein endothelial cells express AnxA3 (*20*). AnxA3- and SE-1-positive cells were observed in normal rat liver section (Fig. 9 panel A and B, respectively), with localization of AnxA3-positive cells corresponding to SE-1-positive cells (Fig. 9, panel C).

Effect of Anti-HGF Antibody on AnxA3 mRNA Level in Hepatocytes Following CCl_4 Treatment—To investigate whether HGF is involved in the increase in AnxA3 mRNA level in hepatocytes following CCl_4 treatment, effect of anti-HGF antibody on mRNA level was investigated. Anti-HGF antibody decreased AnxA3 mRNA level to ~60% compared to control IgG (Fig. 10).

DISCUSSION

In the present study, we demonstrate that expression of AnxA3 increases in two rat liver regeneration models and in parenchymal hepatocytes, but not non-parenchymal liver cells. AnxA3 protein levels in the liver increased at 5 h and 6 h in partially hepatectomized rats and rats treated with CCl_4, respectively. DNA synthesis begins to change at ~16 and 24 h in partially hepatectomized rats and rats treated with CCl_4, respectively (*24*). AnxA3 plays an important role in the signalling cascade in hepatocyte growth for cultured rat hepatocytes (*10*), therefore is also likely to have the same role in rat liver regeneration.

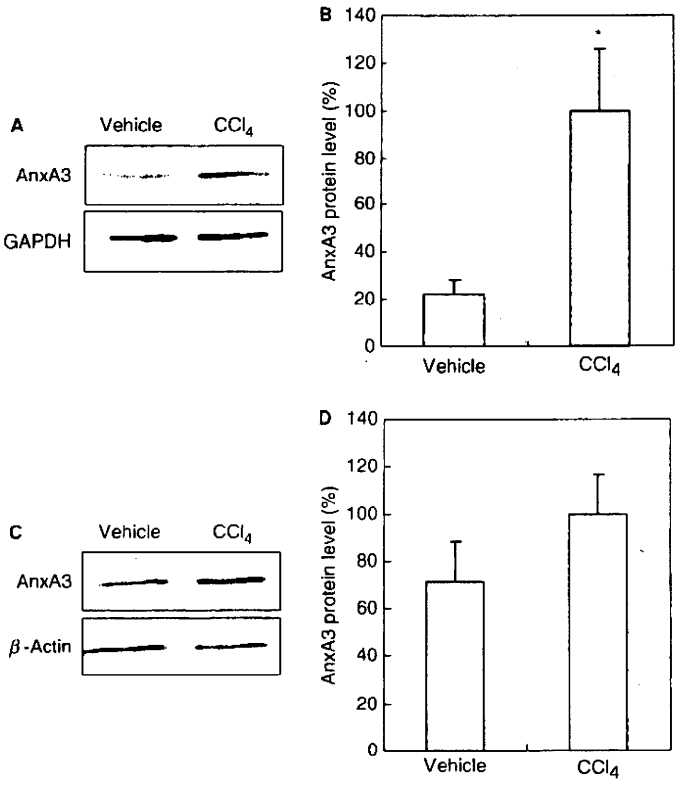

Fig. 3. **AnxA3 protein level in parenchymal hepatocytes and non-parenchymal cells isolated from liver in rats following treatment with CCl_4.** (A) Parenchymal hepatocytes and (C) non-parenchymal cells were isolated from liver in rats at 6 h after either CCl_4 or olive oil treatment. Data shown are representative western blot analysis results for parenchymal hepatocytes and non-parenchymal cells, respectively. Approximately 90 and 0.94 μg of protein was used for the detection of AnxA3 and GAPDH in parenchymal hepatocytes, respectively. Approximately 2.8 μg of protein was used for detection of AnxA3 and beta-actin in non-parenchymal cells. Results for parenchymal hepatocytes (B) and non-parenchymal cell (D) are presented relative to parenchymal hepatocytes and non-parenchymal liver cells from rats at 6 h after CCl_4 administration, respectively. AnxA3 protein levels in parenchymal hepatocytes and non-parenchymal liver cells were normalized to housekeeping protein, GAPDH and beta-actin, respectively. Data are expressed as mean ± SD ($n = 4$) $^*P < 0.01$, compared to the value for parenchymal hepatocytes or non-parenchymal liver cells from rats at 6 h after olive oil treatment.

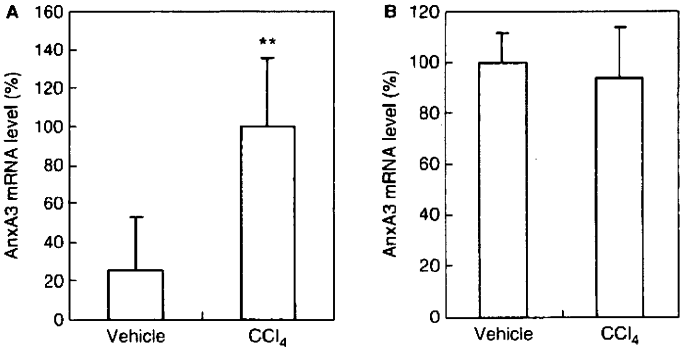

Fig. 4. **AnxA3 mRNA level in parenchymal hepatocytes and non-parenchymal cells isolated from livers in rats following treatment with CCl_4.** (A) Parenchymal hepatocytes and (B) non-parenchymal liver cells were isolated from liver in rats at 6 h after either CCl_4 or olive oil treatment. AnxA3 levels were normalized to the housekeeping gene, 28S rRNA. Results for parenchymal hepatocytes and non-parenchymal liver cells are presented relative to hepatocytes and non-parenchymal cells from rats at 6 h after CCl_4 treatment, respectively. Data are expressed as the mean ± SD ($n = 4$) $^*P < 0.05$, compared to parenchymal hepatocytes and non-parenchymal liver cells from liver in rats at 6 h after olive oil treatment.

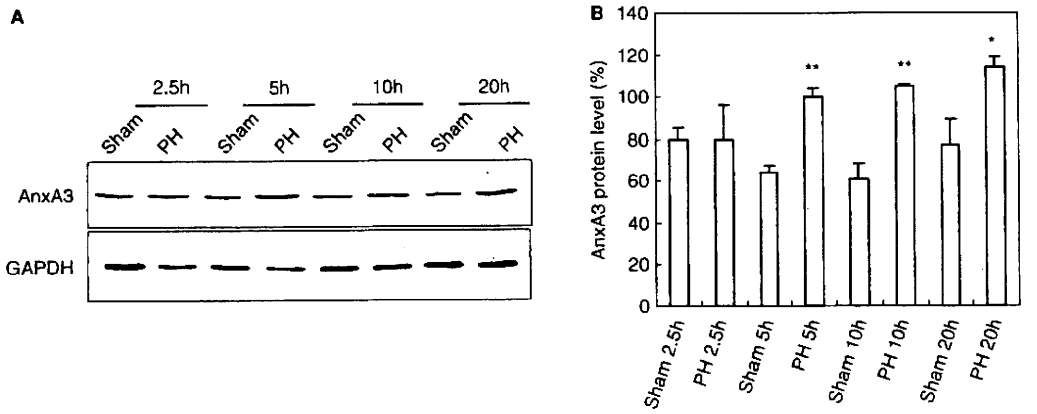

Fig. 5. **AnxA3 protein level in liver after partial hepatectomy.** (A) Data shown are representative of western blot analysis results. Approximately 35 and 1.5 μg of protein were used for detection of AnxA3 and GAPDH, respectively. (B) Results are presented relative to the values for liver in rats at 5 h after partial hepatectomy. AnxA3 protein levels were normalized to levels of housekeeping protein, GAPDH. Data are expressed as mean ± SD ($n = 4$ at each time point) $^{*}P < 0.01$, $^{**}P < 0.05$, compared to the value produced by liver in rats after sham operation.

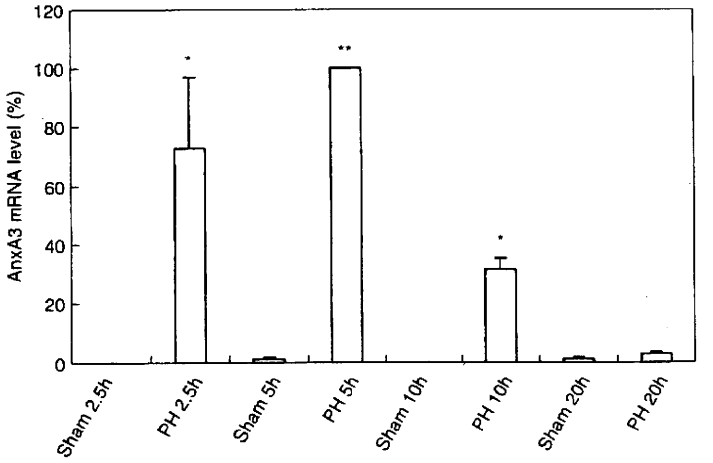

Fig. 6. **AnxA3 mRNA level in liver after partial hepatectomy.** Results are presented relative to the value produced by liver in rats at 5 h after partial hepatectomy. AnxA3 mRNA levels were normalized to housekeeping gene, 28S rRNA. Data are expressed as mean ± SD ($n = 4$ at each time point) $^{*}P < 0.01$, $^{**}P < 0.05$, compared to after sham operation.

Extent of increase in AnxA3 protein level was lower than in AnxA3 mRNA level in rat liver regeneration models, suggesting that AnxA3 protein, for which synthesis is enhanced, degrades rapidly in these conditions. Several proteases are induced or activated in rat liver regeneration (*25–31*). Therefore, AnxA3 may be rapidly degraded by some of these proteases, resulting in the relatively low level of increase in AnxA3 protein expression compared to mRNA expression.

AnxA3 in the liver from rats at 24 h after CCl_4 treatment was investigated using immunohistochemical analysis, to determine whether proliferating cells are AnxA3-positive parenchymal cells. AnxA3 was not detected in parenchymal hepatocytes, but was detected in non-parenchymal liver cells (data not shown). This failure of detection in parenchymal hepatocytes may be because expression of AnxA3 in these cells is too low to detect compared to non-parenchymal liver cells.

AnxA3 protein level increased in hepatocytes after partial hepatectomy; however, AnxA3 mRNA level after sham operation was even higher than after partial hepatectomy, inconsistent with the results for AnxA3 protein level. AnxA3 protein levels did, however, correlate with AnxA3 mRNA levels in cultured rat hepatocytes (*14*). AnxA3 mRNA was undetectable in hepatocytes from normal rats that were not sham operated (*10*, *12*). Therefore, sham operation may induce some signal that leads to an increase in AnxA3

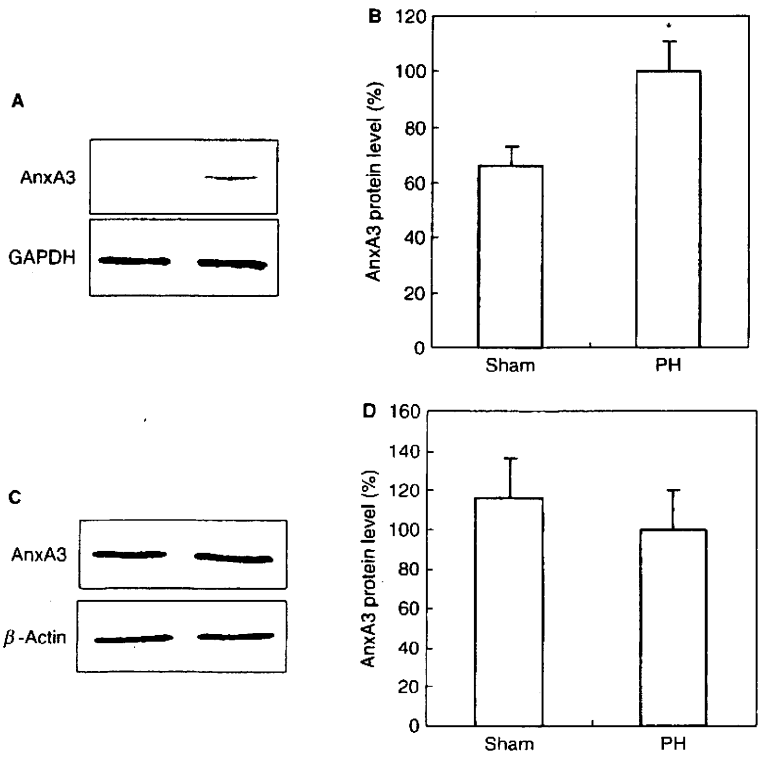

Fig. 7. **AnxA3 protein level in parenchymal hepatocytes and non-parenchymal liver cells after hepatectomy.** (A) Parenchymal hepatocytes and (C) non-parenchymal liver cells were isolated at 5 h after partial hepatectomy or sham operation. Data shown are representative of western blot analysis results for parenchymal hepatocytes and non-parenchymal liver cells, respectively. Approximately 90 and 2.8 μg of protein were used for detection of AnxA3 and GAPDH in parenchymal hepatocytes, respectively. Approximately 2.8 μg of protein was used for detection of AnxA3 and beta-actin in non-parenchymal liver cells. AnxA3 protein levels in parenchymal hepatocytes and non-parenchymal liver cells were normalized to housekeeping proteins GAPDH and beta-actin, respectively. Results for parenchymal hepatocytes (B) and non-parenchymal liver cells (D) are presented relative to the value produced by parenchymal hepatocytes and non-parenchymal liver cells from rats at 5 h after partial hepatectomy, respectively. Data are expressed as mean ± SD ($n = 4$) $^{**}P < 0.01$, compared to parenchymal hepatocytes and non-parenchymal liver cell from rats at 5 h after sham operation.

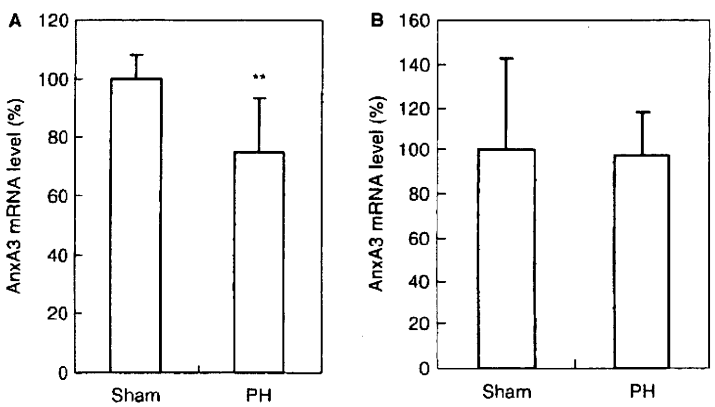

Fig. 8. **AnxA3 mRNA level in parenchymal hepatocytes and non-parenchymal liver cells after partial hepatectomy.** (A) Parenchymal hepatocytes and (B) non-parenchymal liver cells were isolated from liver in rats at 5 h after either partial hepatectomy or sham operation. AnxA3 mRNA levels were normalized to housekeeping gene, 28S rRNA. Results for parenchymal hepatocytes and non-parenchymal liver cells are presented relative to parenchymal hepatocytes and non-parenchymal liver cells from rats at 5 h after partial hepatectomy, respectively. Data are expressed as mean ± SD ($n = 4$) $^{**}P < 0.05$, compared to parenchymal hepatocytes and non-parenchymal liver cells from rats at 5 h after sham operation.

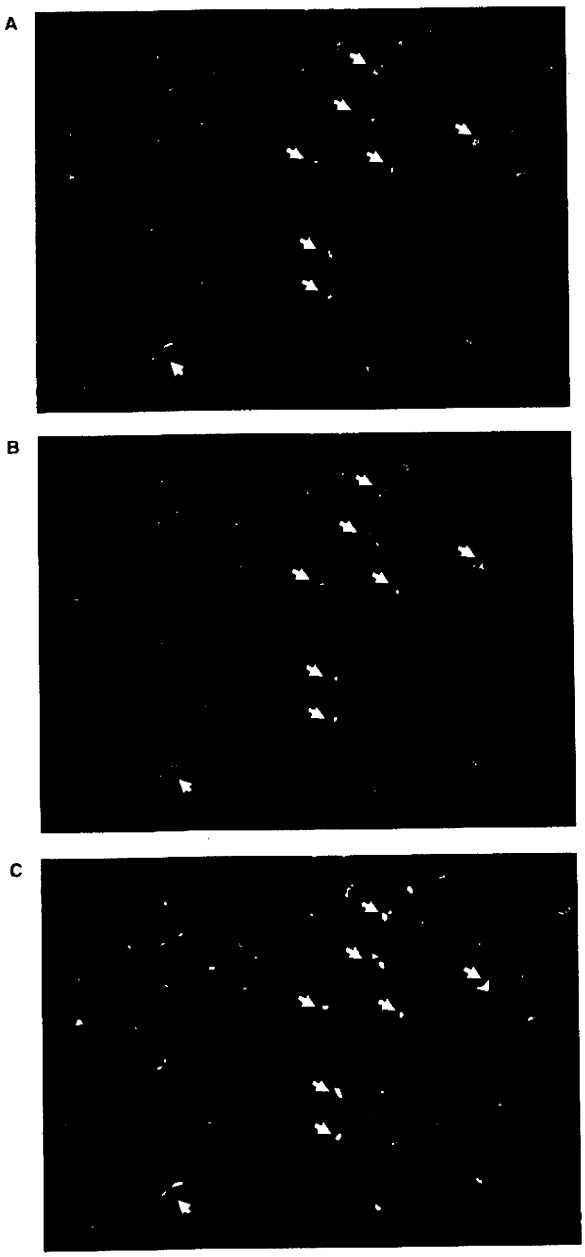

Fig. 9. **AnxA3 expression in hepatic sinusoidal endothelial cells in normal rat liver.** (A) AnxA3-positive cells; (B) SE-1-positive cells; (C) Merged image of AnxA3- and SE-1-positive cells. In (A–C), arrows show examples of positive immunoreactive cells.

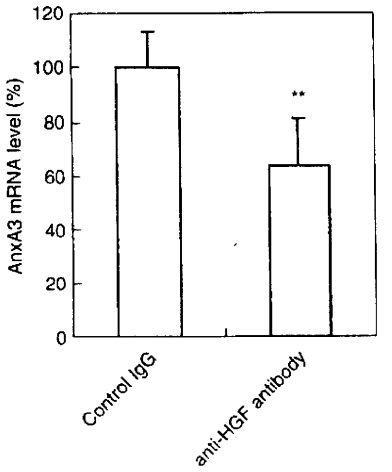

Fig. 10. **Effect of anti-HGF antibody on AnxA3 mRNA level in parenchymal hepatocytes following treatment with CCl_4.** Hepatocytes were isolated from liver in rats at 6 h following treatment with either anti-HGF IgG or control IgG, then CCl_4. AnxA3 levels were normalized to housekeeping gene, 28S rRNA. Results are presented relative to the value produced by hepatocyte isolated from liver in rats at 6 h following treatment with control IgG, then CCl_4. Data are expressed as mean ± SD ($n = 4$) $^{**}P < 0.05$, compared to hepatocytes from rats at 6 h following treatment with control IgG, then CCl_4.

mRNA level only in hepatocyte isolation procedures, including perfusion with collagenase at 37°C. This possibility may be supported by the finding that AnxA3 mRNA level is greatly enhanced in the liver from rats after partial hepatectomy, compared to after sham operation in analysis using total RNA directly extracted from liver perfused with cold PBS.

Increase in AnxA3 mRNA level was inhibited by anti-HGF antibody in hepatocytes from rats at 6 h after CCl_4 administration, indicating that HGF is involved in increasing AnxA3 mRNA expression in hepatocytes. Consistent with this finding, HGF increased AnxA3 mRNA level in hepatocytes cultured on Matrigel (*14*), on which hepatocytes maintain functions similar to those within a normal animal (*32*). HGF protein needs to increase in blood within 6 h at the latest after CCl_4 administration for HGF to increase AnxA3 mRNA level. This was indicated by the finding that HGF protein dramatically rises in the plasma at 2 h after partial hepatectomy and CCl_4 administration (*33*).

Effect of anti-HGF antibody on AnxA3 protein level was investigated; however, reproducible results were not obtained for AnxA3 and GAPDH protein levels in the experiments using control IgG and anti-HGF IgG antibodies. Also, there was a decreased recovery of total protein compared to the parenchymal hepatocytes isolated from liver in rats without these treatments. As administration of IgG was performed only *via* tail vein in this experiment, this procedure may be a factor in this variation. It is likely that the increases in fluid pressure to liver cause liver injury followed by enhancement of protein degradation by some proteases. This is supported by the finding that alanine transaminase transiently elevates in serum from rats after administration of PBS *via* the tail vein (*34*). However, strict control of fluid pressure is difficult in practice. Therefore, variation in

these sequential cascades may result in no reproducible results.

AnxA3 was demonstrated to be expressed in non-parenchymal liver cells, although proteins levels do not change in the liver regeneration models. Further immunohistochemical analysis showed co-localization of AnxA3-positive and SE-1-positive cells indicating that AnxA3 is expressed in hepatic sinusoidal endothelial cells.

In conclusion, the results of this study demonstrate that AnxA3 expression increases in hepatocytes through an HGF-mediated pathway in rat liver regeneration models, suggesting that AnxA3 plays an important role in the signalling cascade in rat liver regeneration.

This work is supported in part by the Grant-in-Aid for Cancer Research (15-2) from the Ministry of Health, Labor and Welfare. We wish to thank Mr Toshihiro Akiyama (Sankyo Labo Service Co.) and Dr Yukio Kodama (Division of Toxicology, National Institute of Health Sciences) for their technical assistance.

REFERENCES

1. Crumpton, M.J. and Dedman, J.R. (1990) Protein terminology tangle. *Nature* **345**, 212
2. Gerke, V. and Moss, S.E. (2002) Annexins: from structure to function. *Physiol. Rev.* **82**, 331–371
3. Moss, S.E. and Morgan, R.O. (2004) The annexins. *Genome Biol.* **5**, 219.211–219.218
4. Raynal, P. and Pollard, H.B. (1994) Annexins: the problem of assessing the biological role for a gene family of multifunctional calcium- and phospholipid-binding proteins. *Biochim. Biophys. Acta* **1197**, 63–93
5. Ernst, J.D., Hoye, E., Blackwood, R.A., and Jaye, D. (1990) Purification and characterization of an abundant cytosolic protein from human neutrophils that promotes Ca2(+)-dependent aggregation of isolated specific granules. *J. Clin. Invest.* **85**, 1065–1071
6. Tait, J.F., Sakata, M., McMullen, B.A., Miao, C.H., Funakoshi, T., Hendrickson, L.E., and Fujikawa, K. (1988) Placental anticoagulant proteins: isolation and comparative characterization four members of the lipocortin family. *Biochemistry* **27**, 6268–6276
7. Ernst, J.D. (1991) Annexin III translocates to the peripheagosomal region when neutrophils ingest opsonized yeast. *J. Immunol.* **146**, 3110–3114
8. Konishi, H., Namikawa, K., and Kiyama, H. (2006) Annexin III implicated in the microglial response to motor nerve injury. *Glia* **53**, 723–732
9. Le Cabec, V., Russo-Marie, F., and Maridonneau-Parini, I. (1992) Differential expression of two forms of annexin 3 in human neutrophils and monocytes and along their differentiation. *Biochem. Biophys. Res. Commun.* **189**, 1471–1476
10. Niimi, S., Harashima, M., Gamou, M., Hyuga, M., Seki, T., Ariga, T., Kawanishi, T., and Hayakawa, T. (2005) Expression of annexin A3 in primary cultured parenchymal rat hepatocytes and inhibition of DNA synthesis by suppression of annexin A3 expression using RNA interference. *Biol. Pharm. Bull.* **28**, 424–428
11. Park, J.E., Lee, D.H., Lee, J.A., Park, S.G., Kim, N.S., Park, B.C., and Cho, S. (2005) Annexin A3 is a potential angiogenic mediator. *Biochem. Biophys. Res. Commun.* **337**, 1283–1287
12. Niimi, S., Hyuga, M., Harashima, M., Seki, T., Ariga, T., Kawanishi, T., and Hayakawa, T. (2004) Isolated small rat hepatocytes express both annexin III and terminal differentiated hepatocyte markers, tyrosine aminotransferase and tryptophan oxygenase, at the mRNA level. *Biol. Pharm. Bull.* **27**, 1864–1866
13. Niimi, S., Oshizawa, T., Yamaguchi, T., Harashima, M., Seki, T., Ariga, T., Kawanishi, T., and Hayakawa, T. (2003) Specific expression of annexin III in rat-small-hepatocytes. *Biochem. Biophys. Res. Commun.* **300**, 770–774
14. Harashima, M., Niimi, S., Koyanagi, H., Hyuga, M., Noma, S., Seki, T., Ariga, T., Kawanishi, T., and Hayakawa, T. (2006) Change in annexin A3 expression by regulatory factors of hepatocyte growth in primary cultured rat hepatocytes. *Biol. Pharm. Bull.* **29**, 1339–1343
15. de Coupade, C., Gillet, R., Bennoun, M., Briand, P., Russo-Marie, F., and Solito, E. (2000) Annexin 1 expression and phosphorylation are upregulated during liver regeneration and transformation in antithrombin III SV40T large antigen transgenic mice. *Hepatology* **31**, 371–380
16. Masaki, T., Tokuda, M., Fujimura, T., Ohnishi, M., Tai, Y., Miyamoto, K., Itano, T., Matsui, H., Watanabe, S., Sogawa, K., Yamada, R., Konishi, M., and Nishioka, A. (1994) Involvement of annexin I and annexin II in hepatocyte proliferation: can annexins I and II be markers for proliferative hepatocytes? *Hepatology* **20**, 425–435
17. Higgins, G.M. and Anderson, R.M. (1931) Experimental pathology of the liver. I. Restration of the liver of the white rat following partial surgical removal. *Arch. Pathol.* **12**, 186–202
18. Tanaka, K., Sato, M., Tomita, Y., and Ichihara, A. (1978) Biochemical studies on liver functions in primary cultured hepatocytes of adult rats. I. Hormonal effects on cell viability and protein synthesis. *J. Biochem. (Tokyo)* **84**, 937–946
19. Shimaoka, S., Nakamura, T., and Ichihara, A. (1987) Stimulation of growth of primary cultured adult rat hepatocytes without growth factors by coculture with nonparenchymal liver cells. *Exp. Cell Res.* **172**, 228–242
20. Romisch, J., Schuler, E., Bastian, B., Burger, T., Dunkel, F.G., Schwinn, A., Hartmann, A.A., and Paques, E.P. (1992) Annexins I to VI: quantitative determination in different human cell types and in plasma after myocardial infarction. *Blood Coagul. Fibrinolysis* **3**, 11–17
21. Bradford, M.M. (1976) A rapid and sensitive method for the quantitation of microgram quantities of protein utilizing the principle of protein-dye binding. *Anal. Biochem.* **72**, 248–254
22. Chomczynski, P. and Sacchi, N. (1987) Single-step method of RNA isolation by acid guanidinium thiocyanate-phenol-chloroform extraction. *Anal. Biochem.* **162**, 156–159
23. Puissant, C. and Houdebine, L. M. (1990) An improvement of the single-step method of RNA isolation by acid guanidinium thiocyanate-phenol-chloroform extraction. *Biotechniques* **8**, 148–149
24. Goyette, M., Petropoulos, C.J., Shank, P.R., and Fausto, N. (1983) Expression of a cellular oncogene during liver regeneration. *Science* **219**, 510–512
25. Goldshmidt, O., Yeikilis, R., Mawasi, N., Paizi, M., Gan, N., Ilan, N., Pappo, O., Vlodavsky, I., and Spira, G. (2004) Heparanase expression during normal liver development and following partial hepatectomy. *J. Pathol.* **203**, 594–602
26. Haruyama, T., Ajioka, I., Akaike, T., and Watanabe, Y. (2000) Regulation and significance of hepatocyte-derived matrix metalloproteinases in liver remodeling. *Biochem. Biophys. Res. Commun.* **272**, 681–686
27. Kim, T.H., Mars, W.M., Stolz, D.B., and Michalopoulos, G.K. (2000) Expression and activation of pro-MMP-2 and pro-MMP-9 during rat liver regeneration. *Hepatology* **31**, 75–82
28. Maianskaia, N.N., Shcherbakov, V.I., Panin, L.E., and Maianskii, D.N. (1978) Change in the state of the lysosomes in isolated Kupffer cells and hepatocytes in the process of liver reparative regeneration. *Tsitologiia* **20**, 1046–1051
29. Mars, W.M., Liu, M.L., Kitson, R.P., Goldfarb, R.H., Gabauer, M.K., and Michalopoulos, G.K. (1995) Immediate early detection of urokinase receptor after partial

hepatectomy and its implications for initiation of liver regeneration. *Hepatology* **21**, 1695–1701
30. Mayanskii, D.N., Scherbakoff, V.I., Mayanskaya, N.N., and Panin, L.E. (1980) Lysosomal enzyme activity in hepatocytes and Kupffer cells from intact and partially hepatectomized rats. *Biochem. Exp. Biol.* **16**, 309–314
31. Olle, E.W., Ren, X., McClintock, S.D., Warner, R.L., Deogracias, M.P., Johnson, K.J., and Colletti, L.M. (2006) Matrix metalloproteinase-9 is an important factor in hepatic regeneration after partial hepatectomy in mice. *Hepatology* **44**, 540–549
32. Ben-Ze'ev, A., Robinson, G.S., Bucher, N.L., and Farmer, S.R. (1988) Cell-cell and cell-matrix interactions differentially regulate the expression of hepatic and cytoskeletal genes in primary cultures of rat hepatocytes. *Proc. Natl Acad. Sci. USA* **85**, 2161–2165
33. Lindroos, P.M., Zarnegar, R., and Michalopoulos, G.K. (1991) Hepatocyte growth factor (hepatopoietin A) rapidly increases in plasma before DNA synthesis and liver regeneration stimulated by partial hepatectomy and carbon tetrachloride administration. *Hepatology* **13**, 743–750
34. Liu, F., Song, Y., and Liu, D. (1999) Hydrodynamics-based transfection in animals by systemic administration of plasmid DNA. *Gene Ther.* **6**, 1258–1266

Transduction Properties of Adenovirus Serotype 35 Vectors After Intravenous Administration Into Nonhuman Primates

Fuminori Sakurai[1], Shin-ichiro Nakamura[2,3], Kimiyo Akitomo[1], Hiroaki Shibata[2], Keiji Terao[2], Kenji Kawabata[1], Takao Hayakawa[4] and Hiroyuki Mizuguchi[1,5]

[1]*Laboratory of Gene Transfer and Regulation, National Institute of Biomedical Innovation, Ibaraki City, Osaka, Japan;* [2]*Tsukuba Primates Research Center, National Institute of Biomedical Innovation, Tsukuba City, Ibaraki, Japan;* [3]*The Corporation for Production and Research of Laboratory Primates, Tsukuba City, Ibaraki, Japan;* [4]*Pharmaceuticals and Medical Devices Agency, Chiyoda-Ku, Tokyo, Japan;* [5]*Graduate School of Pharmaceutical Sciences, Osaka University, Suita City, Osaka, Japan*

Adenovirus serotype 35 (Ad35) vectors have shown promise as effective gene delivery vehicles. However, the transduction profiles of Ad35 vectors in conventional mice allow only a limited estimation of transduction properties of these vectors, because the mouse analog of the subgroup B Ad receptor, CD46, is restricted to the testis. In order to assess the transduction properties of Ad35 vectors more completely, we performed transduction experiments using cynomolgus monkeys, which ubiquitously express CD46 in a pattern similar to that in humans. *In vitro* transduction experiments demonstrated that cultured cells from the cynomolgus monkey were efficiently transduced with Ad35 vectors. In contrast, after intravenous administration into live monkeys hardly any evidence of Ad35 vector–mediated transduction was found in any of the organs, although Ad35 vector genomes were detected in various organs. Less severe histopathological abnormalities were found in the Ad35 vector–infused monkeys than in the conventional Ad5 vector–injected monkeys. In the latter, serious tissue damage and inflammatory responses, such as hepatocyte necrosis and lymphatic hyperplasia in the colon, were induced. Both Ad35 and Ad5 vectors caused similar hematological changes (increase in $CD3^+$ cells, and decrease in $CD16^+$ cells and $CD20^+$ cells) in peripheral blood cells. These results should provide valuable information for the clinical application of Ad35 vectors.

Received 15 September 2007; accepted 16 January 2007; published online 11 March 2008. doi:10.1038/mt.2008.19

INTRODUCTION

Human adenoviruses (Ads) are nonenveloped, double-stranded DNA viruses that are composed of 51 serotypes.[1,2] Among the 51 serotypes, the conventional Ad vectors that are most widely used, including for human clinical trials, are constructed based on the subgroup C Ad serotype 5 (Ad5). Ad5 vectors have several advantages as gene delivery vehicles, but clinical and preclinical studies have revealed three major disadvantages of Ad5 vectors. First, target cells that are important for gene therapy, including malignant tumor cells and dendritic cells, express nil or insufficient levels of a cellular receptor for Ad5, the coxsackievirus-adenovirus receptor. The transduction efficiencies of Ad5 vectors depend to a large extent on the expression levels of coxsackievirus-adenovirus receptor, leading to refractoriness of coxsackievirus-adenovirus receptor-negative cells to Ad5 vectors.[3] Second, >50% of adults are seropositive for Ad5 because natural infection with Ad5 is common.[4,5] Pre-existing anti-Ad5 antibodies not only largely inhibit Ad5 vector–mediated transduction, but may also enhance the toxicities induced by Ad5 vectors.[6] Third, inflammatory responses are systemically and rapidly induced by intravascular administration of Ad5 vectors, leading to tissue damage, and this can be fatal to the host.[7–10]

In order to address these problems, we as well as others have developed a replication-incompetent subgroup B Ad serotype 35 (Ad35) vector.[11–15] Ad35 vectors utilize human CD46 as a cellular receptor.[16,17] Human CD46 is ubiquitously expressed on almost all human cells, leading to a wide tropism of Ad35 vectors. In addition, pre-existing anti-Ad5 immunity does not hamper Ad35 vector–mediated transduction, and seroprevalence for Ad35 is much lower than that for Ad5 (refs. 13,14). Ad35 vectors have properties that make them very promising prospects for use as transduction vehicles, but the transduction efficiencies of Ad35 vectors in conventional mice are lower than those of Ad5 vectors.[12,14] Conventional mice seem inappropriate as animal models for Ad35 vectors because mouse CD46 is expressed only in the testis.[18] In addition, there is low homology between human CD46 and mouse CD46. We considered that transduction experiments with Ad35 vectors should be performed using nonhuman primates so as to properly evaluate the transduction properties of Ad35 vectors. The CD46 of nonhuman primates is ubiquitously expressed in a similar pattern to humans, and shows high homology to human CD46.[19]

In this study, we examined the transduction profiles of Ad35 vectors after intravenous administration into nonhuman primates, *i.e.*, cynomolgus monkeys. Ad35 vector–induced immune responses and the blood concentrations of Ad35 vectors were

Correspondence: *Hiroyuki Mizuguchi, Laboratory of Gene Transfer and Regulation, National Institute of Biomedical Innovation, 7-6-8 Asagi, Saito, Ibaraki City, Osaka 567-0085, Japan. E-mail: mizuguch@nibio.go.jp*

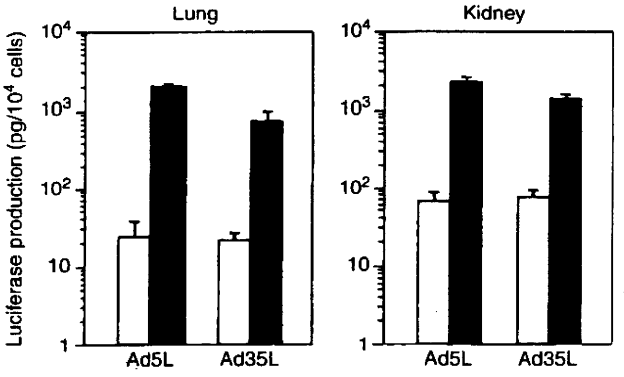

Figure 1 *In vitro* transduction efficiencies of Ad35 and Ad5 vectors in cultured cells of cynomolgus monkey. Luciferase production in primary lung and kidney cells following Ad vector transduction. Primary lung and kidney cells isolated from cynomolgus macaque embryos were transduced with Ad35L or Ad5L at 300 (open bar) and 3,000 vector particles/cell (closed bar) for 1.5 hours. After a 48-hour culture, luciferase production in the cells was measured by luminescence assay. The data are expressed as the mean values ± SD ($n = 4$). Luciferase expression in the mock-infected cells was less than the detectable level. Ad, adenovirus.

analyzed for 4 days after the injection. Necropsy was performed 4 days after the injection to examine the transduction efficiencies, tissue accumulations of Ad35 vectors, and histopathological changes in the organs after injection.

RESULTS

In vitro transduction in cultured cynomolgus monkey cells

First, to examine whether cynomolgus monkey cells were susceptible to Ad35 vectors, primary lung and kidney cells isolated from embryonic cynomolgus monkeys were transduced with a firefly luciferase–expressing Ad35 vector (Ad35L) and a conventional Ad5 vector (Ad5L). Both Ad35L and Ad5L vectors were shown to mediate efficient transduction in the cells from both organs (**Figure 1**). Ad35 vectors also efficiently transduced the cynomolgus monkey T-cell line HSC-F (**Supplementary Figure S1**). These results indicate that cynomolgus monkey cells are susceptible to Ad35 vectors. However, peripheral blood mononuclear cells of cynomolgus monkeys were almost refractory to Ad35 vectors (data not shown).

Blood clearance of Ad vectors

Next, the six cynomolgus monkeys (designated #1–#6) were administered either a β-galactosidase-expressing Ad35 vector (Ad35LacZ) or an Ad5 vector (Ad5LacZ) through the femoral vein (**Supplementary Table S1**). The blood clearances of the Ad vectors were examined using a quantitative real-time polymerase chain reaction. Both Ad35LacZ and Ad5LacZ vectors were rapidly cleared from the blood circulation within 24 hours after the injection (**Figure 2a** and **b**). We did not find any apparent differences between the blood-clearance kinetics of Ad35LacZ and Ad5LacZ. Assuming that the entire Ad vector DNA in the blood was completely recovered from the blood samples, there would remain 0.12% and 0.09% of the injected Ad35LacZ in the blood of monkey #6 at 3 and 6 hours after injection, respectively. The lower levels of

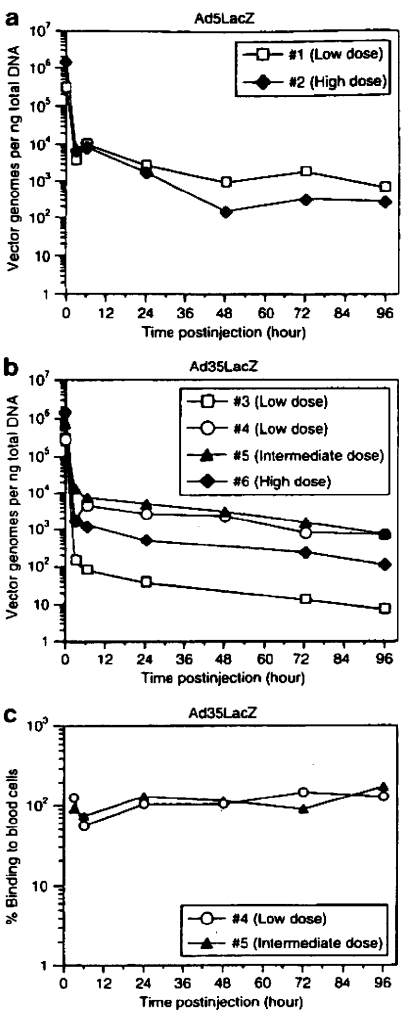

Figure 2 Persistence of adenoviral (Ad) vectors in the blood of cynomolgus monkeys following systemic administration. (**a**) Ad vector DNA concentrations in the blood after intravenous administration. Cynomolgus monkeys were intravenously infused with Ad35LacZ or Ad5LacZ at low [0.4 × 10^{12} vector particles (VP)/kg], intermediate (1.0 × 10^{12}VP/kg), or high (2 × 10^{12}VP/kg) doses. Blood was collected at the indicated time points after injection (3, 6, 24, 48, 72, and 96 hours after injection). Total DNA, including Ad vector DNA, was isolated from the blood, and the Ad vector DNA contents were measured using quantitative TaqMan polymerase chain reaction (PCR) assay. The concentrations of the Ad vectors in the blood at the zero time point were calculated based on the total number of Ad vector particles infused and the estimated circulating blood volume (65 ml/kg). Ad vector DNA was not detected in the blood before injection. (**b**) Percentages of blood cell–associated Ad35lacZ remaining in the blood after systemic administration in cynomolgus monkeys. After isolating the blood as described, blood cells were washed twice with phosphate-buffered saline buffer and the amounts of Ad35LacZ associated with blood cells were evaluated using TaqMan PCR as described earlier. The percentages were calculated as follows: 100 × (the amounts of Ad35 vector DNA associated with blood cells)/(the amounts of Ad35 vector DNA recovered from whole blood).

Ad35LacZ remaining in the blood of monkeys #3 and #6 than those in monkeys #4 and #5 might have been partly because of the low infectious titer-to-particle ratio of the vector batch of Ad35LacZ injected into monkeys #3 and #6. The infectious titer-to-particle

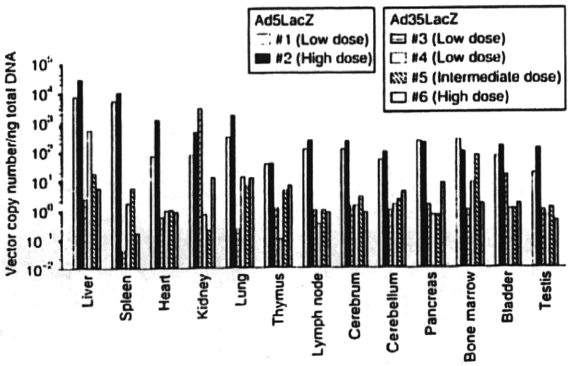

Ad35LacZ or Ad5LacZ was intravenously administered into cynomolgus monkeys as described for **Figure 2**. Four days after the injection, necropsy was performed, and Ad vector DNA contents were measured using quantitative TaqMan polymerase chain reaction analysis. The Ad vector DNA was not detected in the organs of mock-infected animals.

ratio of the Ad35LacZ used in monkeys #3 and #6 was lower than that used in monkeys #4 and #5 (data not shown). Noninfectious Ad particles might be more easily degraded in the blood or taken up by phagocytic cells.

Further, we examined whether the Ad35 vectors were associated with blood cells in the blood stream after the injection. The majority of Ad35LacZ remaining in the blood was associated with blood cells at all the time points (**Figure 2c**). Similarly, assuming the complete recovery of the Ad vector DNA as described earlier, 1.5% of the injected Ad35LacZ would be associated with blood cells in monkey #5 at 3 hours after the injection. The levels of Ad35LacZ associated with blood cells remained constant during the study. These results suggest that Ad35 vectors may bind to blood cells, or be taken up by blood cells after the injection.

Tissue distribution of Ad vectors

In order to examine the biodistribution of Ad35 and Ad5 vectors in cynomolgus monkeys after intravenous administration, Ad DNA contents in the organs were assessed (**Figure 3**). The Ad35 vector DNA was mainly found in the liver, lung, and kidney; however, the levels of Ad35 vector DNA were one to five orders of magnitude lower in almost all organs than the levels of Ad5 vector DNA, which was found mainly in the liver and spleen. Ad35LacZ was also less efficiently accumulated in the organs that exhibited low levels of Ad5LacZ accumulation, such as the thymus and testis.

Ad vector–mediated transgene expression in organs

In order to evaluate the *in vivo* transduction efficiencies of Ad35 and Ad5 vectors, β-galactosidase expression in the organs was examined. Ad5LacZ efficiently transduced the organs (**Figure 4a**). The highest level of β-galactosidase production was found in the liver, followed by the spleen. Liver parenchymal cells and spleen marginal zone cells were mainly transduced by Ad5LacZ in these organs (**Figure 4b**). On the other hand, Ad35 vector–mediated β-galactosidase expression in the organs at all doses was approximately equal to, or slightly above, the levels in

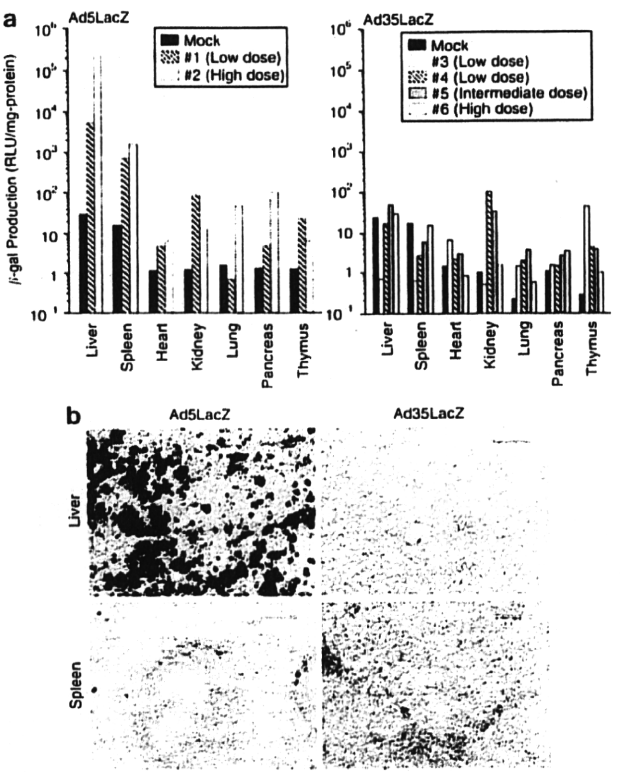

(**a**) Chemiluminescence analysis of β-galactosidase production in cynomolgus monkeys after systemic administration of Ad35LacZ or Ad5LacZ. Ad35LacZ or Ad5LacZ was intravenously injected into cynomolgus monkeys as described for **Figure 2**. Four days after injection, the organs were collected, and β-galactosidase production in the organs was assessed using a chemiluminescence assay. (**b**) X-gal staining of tissue sections of cynomolgus monkeys receiving Ad5LacZ or Ad35LacZ. Four days after intravenous administration of Ad35LacZ or Ad5LacZ at a high dose (2×10^{12} vector particles/kg), tissues were collected, and X-gal staining was performed as described in Materials and Methods. RLU, relative light units.

mock-infected animals. X-gal-positive cells were not found in the tissue sections of the liver or spleen of the Ad35LacZ-infused monkeys. These results indicate that Ad35 vectors show much lower transduction activity than Ad5 vectors after systemic delivery in cynomolgus monkeys.

Serum chemistry profiles

Next, we measured the levels of serum biochemical markers to assess Ad vector–induced tissue/organ damage. Almost all the markers were increased following Ad vector injection; however, overall, the markers examined appeared to be more elevated in the monkeys receiving Ad5LacZ than in those receiving Ad35LacZ (**Figure 5a**). Aspartate aminotransferase (AST) levels were elevated as early as 3 hours after the injection, and peaked at 24 hours in most cases. The peak levels of AST in Ad35LacZ-injected monkeys #3, #4, #5, and #6 were 6.1-, 4.8-, 8.2-, and 3.8-fold higher than the preinjection levels, respectively. By contrast, Ad5LacZ-infused monkeys (#1 and #2) showed 4.9- and 27.5-fold increases in AST at the peak points, respectively. Significant elevations in alanine

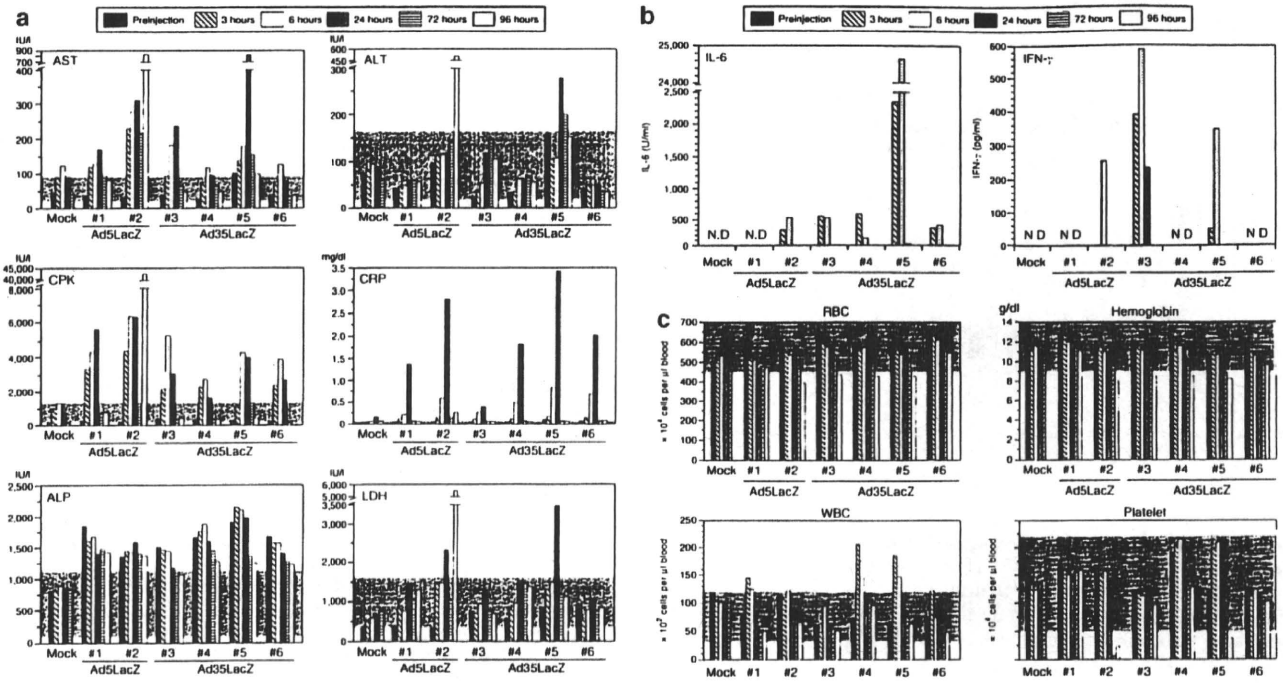

Figure 5 Blood analysis after adenoviral (Ad) vector administration to cynomolgus monkeys. (**a**) Serum marker levels, (**b**) inflammatory cytokine productions, and (**c**) blood cell counts in the peripheral blood after Ad vector administration. The gray area in the graphs of serum markers and blood cell counts indicates the normal range for adult cynomolgus monkeys. Ad35LacZ or Ad5LacZ was intravenously injected into cynomolgus monkeys and blood was collected as described for **Figure 2**. Serum marker levels and blood cell counts were measured using routine methods. Inflammatory cytokine levels were examined using enzyme-linked immunosorbent assay. ALT, alanine aminotransferase; AST, aspartate aminotransferase; CPK, creatine phosphokinase; CRP, C-reactive protein; IFN-γ, interferon-γ; IL-6, interleukin-6; LDH, lactate dehydrogenase; ND, not detected (under the limit of detection); RBC, red blood cell; WBC, white blood cell.

aminotransferase were also found in several of the monkeys, but the alanine aminotransferase levels were within the normal range at almost all the time points. Creatine phosphokinase (CPK) levels sharply rose to a peak 6 or 24 hours after injection. CPK in the Ad35 vector–injected monkeys #3, #4, #5, and #6 showed 14.2-, 9.7-, 16.3-, and 17.7-fold increases at the peak points. On the other hand, the Ad5 vector–injected monkeys #1 and #2 exhibited 16.6- and 40.9-fold elevations in CPK at 6 hours after the injection. Dramatic increases in AST, alanine aminotransferase, and CPK levels in monkey #2 at 96 hours after injection was possibly caused by a slight expression of Ad5 E2 and/or E4 proteins. E4 protein was expressed in the liver 4 days after injection of conventional Ad vectors in mice, leading to liver damage.[20] Levels of C-reactive protein were also sharply increased in all the Ad vector–injected animals. A high dose of Ad35LacZ and Ad5LacZ caused 29-fold (#6) and 56.2-fold (#2) increases in C-reactive protein levels 24 hours after injection, respectively. Alkaline phosphatase levels gradually decreased over the first 96 hours after injection. Alkaline phosphatase levels at preinjection were higher than the normal range in the monkeys. This is because young cynomolgus monkeys (<4 years of age) often have alkaline phosphatase levels >1,000 IU/L. Apparent increases in lactate dehydrogenase were found in monkeys #2 and #5. The lactate dehydrogenase levels in the other animals were within the normal range. There were no abnormalities in the other parameters, including serum albumin, glucose, cholesterol, calcium, sodium, potassium, and chloride (data not shown).

Inflammatory cytokine induction

In order to examine the innate immune responses after Ad vector injection, inflammatory cytokine levels in the serum were measured (**Figure 5b**). Interleukin-6 (IL-6) was rapidly induced with a peak at 3 or 6 hours after the injection in all the animals except in monkey #1. There were no apparent differences in IL-6 levels between Ad35LacZ-treated and Ad5LacZ-treated animals, except that monkey #5 produced an extremely high level of IL-6. The levels of interferon-γ were also elevated and reached a peak at 6 hours after the injection in monkeys #2, #3, and #5. Tumor necrosis factor-α was not detected in any of the animals (data not shown).

Hematological profiles

In order to evaluate the influence of Ad vector injection on the hematological profiles, we examined the changes in peripheral blood cell counts (**Figure 5c**). The changes in the levels of red blood cells and hemoglobin were marginal, but the levels gradually decreased after injection in all the monkeys, including a mock-infected animal, probably because of the collection of large volumes of blood samples (>5 ml/time point) every day. Ad35LacZ-injected monkeys #3, #4, and #5, and Ad5LacZ-injected monkey #2 showed a rapid decline in platelet levels beginning at 24 hours after the injection. A transient increase in the platelet levels was found 3 and 6 hours after the injection in monkey #5. It remains unclear why the platelet levels increased in monkey #5; however, the previous study also reported an initial increase in the platelet levels after Ad5 vector injection in nonhuman primates.[21] A rapid

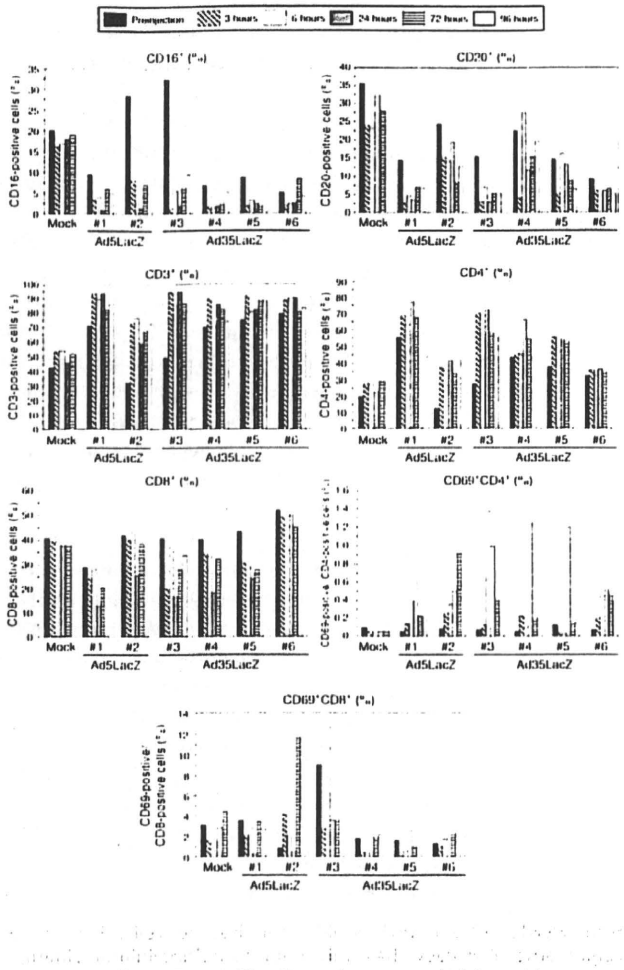

Ad35LacZ or Ad5LacZ was intravenously injected into cynomolgus monkeys and blood was collected as described for **Figure 2**. Peripheral blood mononuclear cells were stained with monoclonal antibodies following hemolysis, and fluorescence-activated cell sorting analysis was performed for evaluation of profiles of lymphocyte subsets.

elevation in the white blood cells was observed in the Ad vector–injected monkeys. The elevated white blood cells level returned to normal at 24 hours after the injection.

Next, we examined which types of blood cells were increased or decreased after Ad vector injection (**Figure 6**). The Ad vector injection induced a rapid decline in the percentages of $CD16^+$ cells (natural killer cells, granulocytes, and monocytes). Monkeys #2 and #3 showed sharp decreases of 71 and 97% of $CD16^+$ cells, respectively, at 3 hours after the injection. The percentages of $CD20^+$ cells (B cells) quickly dropped in all the monkeys, including a mock-infected monkey. In contrast, the $CD3^+$ cell (T-cell) levels were sharply elevated in the animals receiving the Ad vectors. We found a 1.1- to 2.3-fold increase in $CD3^+$ cell levels at 3 hours after the injection. $CD8^+$ cells did not increase, but rather decreased after the injection; however, increases in $CD4^+$ cells were found in the Ad vector–injected monkeys. The $CD4^+$ cell levels were 1.1- to 3.4-fold elevated compared with the preinjection levels, with a peak at 24 hours after the injection, in most of the animals. The administration of Ad vectors also increased

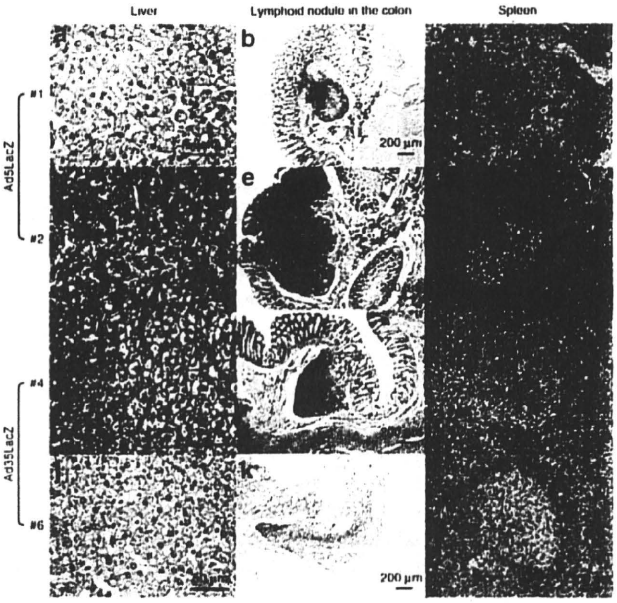

Representative histological sections of the liver (**a**, **d**, **g**, **j**), lymphoid nodules in the colon (**b**, **e**, **h**, **k**), and spleen (**c**, **f**, **i**, **l**) from animals killed 4 days after systemic injection of a low or high dose of Ad35LacZ (monkeys #4 and #6) or Ad5LacZ (#1 and #2). The arrows indicate necrosis of hepatocytes.

$CD69^+CD4^+$ cells (activated $CD4^+$ cells) more predominantly than $CD69^+CD8^+$ cells. Both $CD29^+CD4^+$ cells (memory helper T cells) and $CD29^-CD4^+$ cells (naive helper T cells) increased in the Ad vector–injected animals (data not shown). These results indicate that, overall, both Ad35 and Ad5 vectors cause similar changes in hematological profiles after systemic infusion.

Clinical observation and histopathological examinations

In order to perform a safety assessment of the Ad vectors, the health condition of the animals was monitored until necropsy. None of the Ad vector–infused monkeys showed any apparent abnormalities in appetite, body weight, body temperature, or heart rate. However, the low dose of Ad35LacZ (#3) induced vomiting 3 hours after the injection, and a skin rash was observed in monkey #2 on day 2.

In order to further evaluate the safety profiles of Ad vectors, organ histopathology was examined during necropsy. There were no obvious changes in the spleens of monkeys #1 and #3–#6, or in the livers in any of the animals. However, splenomegaly was found in monkey #2. The whitish nodules at the cut surface of the spleen in monkey #2 were the largest among those of all the monkeys examined. Marked swelling of the lymph nodules, especially in the colon and mesentery, was also found in monkey #2.

Microscopic analysis of tissue sections revealed that no apparent damage and inflammation were found in the liver of monkey #1 (**Figure 7a**). Although slight hyperplasia in the spleen white pulp occurred in this monkey (**Figure 7c**), no obvious changes were found in the lymphatic nodules of the colon (**Figure 7b**). In contrast, severe damage and inflammation, including necrosis of hepatocytes (**Figure 7d**, arrows) and infiltration of lymphocytes

into the Glisson's sheath (data not shown) were found in monkey #2. Furthermore, apparent severe hyperplasia in the lymphoid nodules of the colon (**Figure 7e**) and spleen white pulp (**Figure 7f**) had been induced in monkey #2. On the other hand, the livers of Ad35LacZ-treated monkeys exhibited almost no damage or inflammation (**Figure 7g** and **j**). In addition, Ad35LacZ induced hyperplasia in lymphoid nodules of the colon (**Figure 7h** and **k**) was only slightly developed and less serious than that induced by the high dose of Ad5LacZ. These results suggest that Ad5 vectors may cause more severe damage and/or inflammation in the liver and lymphoid nodules of the colon than Ad35 vectors. The spleen white pulp developed only slight hyperplasia in monkey #4 (**Figure 7i**), in contrast, the high dose of Ad35LacZ induced severe hyperplasia in the spleen white pulp (**Figure 7l**). The level of hyperplasia in spleen white pulp of monkey #6 appeared to be slightly more severe than that of monkey #2. The monkeys #3 and #5 did not show apparent abnormalities in the spleen or colon, although slight vacuolation in hepatocytes and infiltration of lymphocytes in the Glisson's sheath was found (data not shown). Hyperplasia in spleen white pulp and lymphatic follicles in the mesenteric, axillary, and inguinal lymph nodes (data not shown) occurred dose-dependently in the Ad35-injected animals as well as in the Ad5-injected ones.

DISCUSSION

In this study, subgroup B Ad35 vectors were intravenously infused into cynomolgus monkeys in order to evaluate the *in vivo* fundamental transduction properties of Ad35 vectors more thoroughly. Cynomolgus monkey CD46 and the CD46 of other nonhuman primates, have significant homology with human CD46 (ref. 19). In particular, short consensus repeats 1 and 2 (which are crucial for Ad35 binding to CD46),[22–24] of the CD46 of the cynomolgus monkey show high homology (85%) with those in human CD46. In addition, we confirmed that the monkey cells used in this study were highly stained with anti-human CD46 monoclonal antibody M177, which is specific for short consensus repeat 2, and that the antibody M177 significantly inhibited Ad35 vector-mediated transduction in the cynomolgus monkey cells (data not shown). The amino acid sequences important for Ad35 binding to CD46 (refs. 23,24) are also well conserved in cynomolgus monkey CD46. These results indicate that cynomolgus monkey CD46 serves as a cellular receptor for Ad35, at least in the context of *in vitro* transduction.

In this study, four and two cynomolgus monkeys were intravenously injected with the Ad35 and Ad5 vectors, respectively. We must exercise caution in interpreting the results because the sample size is small, as is natural in nonhuman primate studies. Overall, there are no dose responses in several transduction profiles of both Ad35 and Ad5 vectors, including blood concentration of Ad vectors and inflammatory cytokine production. The variations in the transduction profiles suggest that these profiles may depend largely on the specific Ad vector batch and on the differences between individuals, such as health conditions and genetic backgrounds, as well as on Ad vector doses. In the clinical trials using Ad vectors, inflammatory responses were dramatically different between patients receiving the same vector dose.[10] Gene therapy studies, both preclinical and clinical, should be performed with considerable caution in view of these individual differences. Further studies, including toxicogeomics, would be necessary in order to clarify which parameters play the most crucial roles in this entire process of transduction. Such studies would enable prediction of profiles of Ad vector–mediated transduction, and associated toxicities.

Although efficient transduction was achieved using Ad35 vectors *in vitro*, transduction of Ad35 vectors in the organs *in vivo* was hardly detectable after systemic infusion (**Figure 4**). In addition, the levels of Ad35 vector genome in the organs were one to five orders lower than those of the Ad5 vector genome (**Figure 3**). Previous studies demonstrated that, after systemic injection, Ad35 vectors were poor at transducing CD46-transgenic (CD46TG) mice, which ubiquitously express human CD46 in all the organs.[25,26] Chimeric Ad5 vectors containing Ad35 fiber protein also mediated much lower transgene expression in baboons than conventional Ad5 vectors did.[27] These results indicate that Ad35 vectors cannot transduce organs efficiently when introduced into the blood stream. There are two possible explanations for the poor transduction activity of Ad35 vectors after systemic administration. First, Ad35 vectors might be more susceptible than Ad5 vectors to degradation in the blood or in intracellular compartments such as endosomes/lysosomes after internalization. Fiber-substituted Ad5 vectors containing a fiber protein of Ad35 remain for a longer time in late endosome/lysosomal compartments after internalization than Ad5 vectors do.[28] Ad35 vectors might exhibit similar intracellular trafficking to the fiber-substituted Ad5 vectors, leading to high susceptibility to intracellular degradation. Second, Ad35 vectors might not be able to gain access to CD46 after systemic injection. CD46 is predominantly expressed on the basolateral sides of cells,[29,30] making it inaccessible to Ad35 vectors. Ad35 vectors which are not able to bind to CD46 on the cell surface would be phagocytosed into phagocytic cells, such as liver Kupffer cells, leading to degradation.

It is well known that erythrocytes of cynomolgus monkeys express CD46 (ref. 19) and that Ad35 causes hemagglutination of monkey erythrocytes.[31] Ad35 vectors might induce hemagglutination in the blood vessels after the injection, and this might lead to hemolysis and a decrease in the transduction efficiencies of Ad35 vectors. A large percentage of the Ad35 vectors recovered from the blood after the injection were associated with blood cells (**Figure 2c**). However, lactate dehydrogenase (a marker of hemolysis) levels in the sera of Ad35LacZ-injected animals at most of the time points were within normal levels and comparable with those in the sera of animals injected with Ad5LacZ, which does not induce hemagglutination of monkey erythrocytes. These results suggest that hemagglutination by Ad35 vectors would have, at most, a minimal influence on the transduction profiles of Ad35 vectors.

As mentioned earlier, CD46TG mice as well as cynomolgus monkeys were only poorly transduced with Ad35 vectors after intravenous administration, thereby suggesting that the transduction profiles of Ad35 vectors in CD46TG mice would correspond to those in primates and that CD46TG mice might be suitable as a small animal model for the study of Ad35 vectors. The profiles of inflammatory cytokine production by Ad35 vectors in cynomolgus monkeys were also approximately similar to those in CD46TG mice. Intravenous

infusion of Ad35 vectors resulted in levels of inflammatory cytokine production comparable to those induced by Ad5 vectors in the monkeys (**Figure 5b**) as well as in CD46TG mice.[32]

Histopathological analysis demonstrated that tissue damage and inflammatory responses, including hepatocyte necrosis, were less severe in all the Ad35 vector–infused monkeys than in the Ad5 vector–injected ones (**Figure 7**). Previous studies also demonstrated that Ad35 vectors are less immunogenic than Ad5 vectors in mice,[33,34] and this may result in the higher safety profiles of Ad35 vectors as compared to Ad5 vectors. It remains to be elucidated why Ad35 vectors produce less severe side effects than Ad5 vectors. Ad5 vectors were more widely distributed in most organs than Ad35 vectors, suggesting that Ad5 vectors may cause tissue damage and inflammatory responses throughout the whole body. On the other hand, Ad35LacZ induced much higher levels of IL-6 and interferon-γ in monkeys #5 and #3, respectively, than in the other Ad35LacZ-infused monkeys (**Figure 5b**), although no severe damage or inflammation was observed in these two animals. It remains unclear why such high levels of inflammatory cytokines were induced by Ad35 vectors in these animals; however, previous studies have indicated that the high levels of inflammatory cytokine induction might be involved in tissue damage.[9,35] It is important to pay attention to Ad35 vector–induced innate immune responses.

The poor transduction efficiencies of Ad35 vectors in organs after systemic administration could constitute another potential advantage in their use, namely, that locally administered Ad35 vectors would not cause unwanted side effects in organs other than the targeted organs, when draining from injected sites into the blood stream. This is in contrast to Ad5 vectors which, after injection into local tissues, have been shown to drain into the blood stream in large quantities and cause unwanted side effects in the liver and other organs.[36,37] We previously demonstrated that intramuscular injection of Ad35 vectors led to efficient transduction at the injected sites,[12] and thus local injection of Ad35 vectors would be expected to mediate efficient transduction at the injected sites without side effects in other organs.

In summary, we have demonstrated the transduction properties of Ad35 vectors after intravenous administration in nonhuman primates. Systemic infusion of Ad35 vectors did not result in detectable levels of transgene expression in the organs. Also, the tissue damage was less severe in the animals receiving Ad35 vectors than in those receiving Ad5 vectors, although two monkeys produced marked inflammatory cytokines after receiving Ad35 vectors. Further studies are in progress, focusing on the local injection of Ad35 vectors, and the results of these studies may further clarify the potential utility of Ad35 vectors.

MATERIALS AND METHODS

Ad vectors. An Ad5 vector and an Ad35 vector containing a β-galactosidase expression cassette, Ad5LacZ and Ad35LacZ, respectively, were prepared using an improved *in vitro* ligation method.[38–40] Briefly, for preparation of Ad5LacZ, pHMCMV6-LacZ, which was constructed by insertion of the β-galactosidase gene derived from pCMVβ (Clontech, Palo Alto, CA) into pHMCMV6,[39] was digested with I-*Ceu*I and PI-*Sce*I, and then ligated with I-*Ceu*I- and PI-*Sce*I-digested Ad5 vector plasmid pAdHM4.[39] The resulting plasmid was digested with *Pac*I and transfected into 293 cells with Superfect (Qiagen, Valencia, CA). The vector plasmid for Ad35LacZ was constructed in a similar manner, but using pHMCMV6-LacZ and pAdMS18.[25] The resulting plasmid was digested with *Sbf*I and transfected into 293-E1B cells,[25] which are a 293 transformant stably expressing Ad35 E1B-55K protein. The viruses were prepared using a standard method, and purified by $CsCl_2$ step gradient ultracentrifugation followed by $CsCl_2$ linear gradient ultracentrifugation. Determination of virus particle titers was accomplished spectrophotometrically using the methods of Maizel *et al.*[41] Luciferase-expressing Ad5 and Ad35 vectors, Ad5L and Ad35L, were constructed as explained earlier.[11]

In vitro *transduction.* Lung and kidney primary cells, isolated from embryonic cynomolgus monkeys and cultured in Roswell Park Memorial Institute-1640 medium supplemented with 10% fetal bovine serum, antibiotics, and L-glutamine, were seeded in a 96-well dish at 1×10^4 cells/well. On the following day, they were transduced with Ad5L or Ad35L at 300 and 3,000 vector particles/cell for 1.5 hours. After a 48-hour culture period, luciferase production in the cells was measured using a luciferase assay system (PicaGene LT2.0; Toyo Inki, Tokyo, Japan).

Animals. Young male cynomolgus monkeys (*Macaca fascicularis*) were housed and handled in accordance with the rules for animal care and management of the Tsukuba Primate Center and the guiding principles for animal experiments using nonhuman primates formulated by the Primate Society of Japan. The animals (~3 years of age, 1.88–2.96 kg) were certified free of intestinal parasites and seronegative for simian type-D retrovirus, herpesvirus B, varicella-zoster-like virus, and measles virus. The protocol of the experimental procedures was approved by the Animal Welfare and Animal Care Committee of the National Institute of Biomedical Innovation (Osaka, Japan).

In vivo *transduction.* Cynomolgus monkeys were sedated with ketamine (5–10 mg/kg) and injected with phosphate-buffered saline (mock), or Ad5LacZ or Ad35LacZ at 2×10^{12} vector particles/kg (high dose), 1×10^{12} vector particles/kg (intermediate dose), or 0.4×10^{12} vector particles/kg (low dose) through the saphenous vein at a rate of ~2 ml/minutes. Blood was collected for analysis at 3, 6, 24, 48, 72, and 96 hours after injection. Four days after vector administration, the monkeys were killed and the tissues were collected. Tissue samples were subjected to analysis as described in the later text.

β-Galactosidase assay and X-gal staining. β-Galactosidase activity in the organs was measured using Galacto-Light Systems (Applied Biosystems, Foster City, CA) as earlier described.[42] Protein concentrations were determined with a Bio-Rad assay kit (Bio-Rad, Hercules, CA) using bovine serum albumin as a standard. X-gal staining of tissue sections was performed as earlier described.[43]

Blood clearance and tissue distribution of Ad vectors. Blood clearance analysis of Ad vectors was performed using a real-time polymerase chain reaction assay, as earlier described.[8,40] Briefly, total DNA, including the Ad vector DNA, was isolated from whole blood samples. After isolation, the total DNA concentrations were determined, and the Ad DNA contents were quantified using a TaqMan fluorogenic detection system (ABI Prism 7700 sequence detector; Perkin-Elmer Applied Biosystems, Foster City, CA).

The association of Ad35 vectors to blood cells circulating in the blood stream was evaluated using a real-time polymerase chain reaction assay. Blood samples collected at the indicated time points were washed two times with phosphate-buffered saline immediately after isolation to remove unbound Ad35 vectors. After washing, total DNA was extracted from blood cells and the Ad35 DNA contents were assessed as described earlier.

The Ad DNA contents in each organ were similarly quantified using a real-time polymerase chain reaction assay, as described earlier, after isolation of the total DNA from each organ using a Automatic Nucleic Acid Isolation System (NA-2000; KURABO, Osaka, Japan).

Histopathology. For routine histopathology, tissues were fixed in 10% formalin at the time of necropsy, and processed for paraffin embedding.

Sections of 4-μm thickness were cut and stained with hematoxylin and eosin. The tissue sections were examined under a microscope.

Analysis of inflammatory cytokines, serum chemistry profiles, and hematology parameters. Blood was drawn from the saphenous veins of all the monkeys prior to vector administration and at 3, 6, 24, 72, and 96 hours after vector administration. Blood samples were collected into separate tubes containing either EDTA or no anticoagulant, for hematology and for determination of inflammatory cytokines and serum chemistry, respectively. Serum samples for analysis of inflammatory cytokines and serum chemistry were separated by centrifugation (4 °C, 2,500 rpm, 15 minutes), stored in a freezer at −80 °C, and thawed at the time of measurement. The levels of inflammatory cytokines (IL-6 and interferon-γ) in serum samples were measured using enzyme-linked immunosorbent assay (BioSource, Camarillo, CA). The serum chemistry parameters, which were measured with an automated chemistry analyzer AU400 (OLYMPUS, Tokyo, Japan), included AST, alanine aminotransferase, CPK, alkaline phosphatase, lactate dehydrogenase, and C-reactive protein. The hematology parameters that were determined included white blood cells, red blood cells, hemoglobin, platelets, $CD3^+$ cells, $CD4^+$ cells, $CD8^+$ cells, $CD16^+$ cells, $CD20^+$ cells, $CD29^+$ cells, and $CD69^+$ cells.

ACKNOWLEDGMENTS

The authors thank Fumiko Ono and Chieko Ohno (The Corporation for Production and Research of Laboratory Primates, Tsukuba City, Ibardki, Japan) for their help. This work was supported by grants from the Ministry of Health, Labour, and Welfare of Japan and a Grant-in-Aid for Scientific Research on Priority Areas of the Ministry of Education, Culture, Sports, Science, and Technology (MEXT) of Japan.

SUPPLEMENTARY MATERIAL

Figure S1. *In vivo* transduction efficiencies of Ad35 and Ad5 vectors in cultured cynomolgus monkey T-cell line H-SCF.

Table S1. Dosing of cynomolgus macaques with β-galactosidase-expressing Ad vectors in this study.

REFERENCES

1. Havenga, MJ, Lemckert, AA, Ophorst, OJ, van Meijer, M, Germeraad, WT, Grimbergen, J *et al.* (2002). Exploiting the natural diversity in adenovirus tropism for therapy and prevention of disease. *J Virol* **76**: 4612–4620.
2. De Jong, JC, Wermenbol, AG, Verweij-Uijterwaal, MW, Slaterus, KW, Wertheim-Van Dillen, P, Van Doornum, GJ *et al.* (1999). Adenoviruses from human immunodeficiency virus-infected individuals, including two strains that represent new candidate serotypes Ad50 and Ad51 of species B1 and D, respectively. *J Clin Microbiol* **37**: 3940–3945.
3. Wickham, TJ (2000). Targeting adenovirus. *Gene Ther* **7**: 110–114.
4. Ophorst, OJ, Radosević, K, Havenga, MJ, Pau, MG, Holterman, L, Berkhout, B *et al.* (2006). Immunogenicity and protection of a recombinant human adenovirus serotype 35-based malaria vaccine against *Plasmodium yoelii* in mice. *Infect Immun* **74**: 313–320.
5. Chirmule, N, Propert, K, Magosin, S, Qian, Y, Qian, R and Wilson, J (1999). Immune responses to adenovirus and adeno-associated virus in humans. *Gene Ther* **6**: 1574–1583.
6. Vlachaki, MT, Hernandez-Garcia, A, Ittmann, M, Chhikara, M, Aguilar, LK, Zhu, X *et al.* (2002). Impact of preimmunization on adenoviral vector expression and toxicity in a subcutaneous mouse cancer model. *Mol Ther* **6**: 342–348.
7. Muruve, DA (2004). The innate immune response to adenovirus vectors. *Hum Gene Ther* **15**: 1157–1166.
8. Koizumi, N, Kawabata, K, Sakurai, F, Watanabe, Y, Hayakawa, T and Mizuguchi, H (2006). Modified adenoviral vectors ablated for coxsackievirus-adenovirus receptor, alphav integrin, and heparan sulfate binding reduce *in vivo* tissue transduction and toxicity. *Hum Gene Ther* **17**: 264–279.
9. Koizumi, N, Yamaguchi, T, Kawabata, K, Sakurai, F, Sasaki, T, Watanabe, Y *et al.* (2007). Fiber-modified adenovirus vectors decrease liver toxicity through reduced IL-6 production. *J Immunol* **178**: 1767–1773.
10. Raper, SE, Chirmule, N, Lee, FS, Wivel, NA, Bagg, A, Gao, GP *et al.* (2003). Fatal systemic inflammatory response syndrome in a ornithine transcarbamylase deficient patient following adenoviral gene transfer. *Mol Genet Metab* **80**: 148–158.
11. Sakurai, F, Mizuguchi, H and Hayakawa, T (2003). Efficient gene transfer into human $CD34^+$ cells by an adenovirus type 35 vector. *Gene Ther* **10**: 1041–1048.
12. Sakurai, F, Mizuguchi, H, Yamaguchi, T and Hayakawa, T (2003). Characterization of *in vitro* and *in vivo* gene transfer properties of adenovirus serotype 35 vector. *Mol Ther* **8**: 813–821.
13. Seshidhar Reddy, P, Ganesh, S, Limbach, MP, Brann, T, Pinkstaff, A, Kaloss, M *et al.* (2003). Development of adenovirus serotype 35 as a gene transfer vector. *Virology* **311**: 384–393.
14. Vogels, R, Zuijdgeest, D, van Rijnsoever, R, Hartkoorn, E, Damen, I, de Béthune, MP *et al.* (2003). Replication-deficient human adenovirus type 35 vectors for gene transfer and vaccination: efficient human cell infection and bypass of preexisting adenovirus immunity. *J Virol* **77**: 8263–8271.
15. Gao, W, Robbins, PD and Gambotto, A (2003). Human adenovirus type 35: nucleotide sequence and vector development. *Gene Ther* **10**: 1941–1949.
16. Gaggar, A, Shayakhmetov, DM and Lieber, A (2003). CD46 is a cellular receptor for group B adenoviruses. *Nat Med* **9**: 1408–1412.
17. Segerman, A, Atkinson, JP, Marttila, M, Dennerquist, V, Wadell, G and Arnberg, N (2003). Adenovirus type 11 uses CD46 as a cellular receptor. *J Virol* **77**: 9183–9191.
18. Tsujimura, A, Shida, K, Kitamura, M, Nomura, M, Takeda, J, Tanaka, H *et al.* (1998). Molecular cloning of a murine homologue of membrane cofactor protein (CD46): preferential expression in testicular germ cells. *Biochem J* **330**: 163–168.
19. Hsu, EC, Sabatinos, S, Hoedemaeker, FJ, Rose, DR and Richardson, CD (1999). Use of site-specific mutagenesis and monoclonal antibodies to map regions of CD46 that interact with measles virus H protein. *Virology* **258**: 314–326.
20. Gao, GP, Yang, Y and Wilson, JM (1996). Biology of adenovirus vectors with E1 and E4 deletions for liver-directed gene therapy. *J Virol* **70**: 8934–8943.
21. Brunetti-Pierri, N, Palmer, DJ, Beaudet, AL, Carey, KD, Finegold, M and Ng, P (2004). Acute toxicity after high-dose systemic injection of helper-dependent adenoviral vectors into nonhuman primates. *Hum Gene Ther* **15**: 35–46.
22. Sakurai, F, Murakami, S, Kawabata, K, Okada, N, Yamamoto, A, Seya, T *et al.* (2006). The short consensus repeats 1 and 2, not the cytoplasmic domain, of human CD46 are crucial for infection of subgroup B adenovirus serotype 35. *J Control Release* **113**: 271–278.
23. Gaggar, A, Shayakhmetov, DM, Liszewski, MK, Atkinson, JP and Lieber, A (2005). Localization of regions in CD46 that interact with adenovirus. *J Virol* **79**: 7503–7513.
24. Fleischli, C, Verhaagh, S, Havenga, M, Sirena, D, Schaffner, W, Cattaneo, R *et al.* (2005). The distal short consensus repeats 1 and 2 of the membrane cofactor protein CD46 and their distance from the cell membrane determine productive entry of species B adenovirus serotype 35. *J Virol* **79**: 10013–10022.
25. Sakurai, F, Kawabata, K, Koizumi, N, Inoue, N, Okabe, M, Yamaguchi, T *et al.* (2006). Adenovirus serotype 35 vector-mediated transduction into human CD46-transgenic mice. *Gene Ther* **13**: 1118–1126.
26. Verhaagh, S, de Jong, E, Goudsmit, J, Lecollinet, S, Gillissen, G, de Vries, M *et al.* (2006). Human CD46-transgenic mice in studies involving replication-incompetent adenoviral type 35 vectors. *J Gen Virol* **87**: 255–265.
27. Ni, S, Bernt, K, Gaggar, A, Li, ZY, Kiem, HP and Lieber, A (2005). Evaluation of biodistribution and safety of adenovirus vectors containing group B fibers after intravenous injection into baboons. *Hum Gene Ther* **16**: 664–677.
28. Shayakhmetov, DM, Li, ZY, Ternovoi, V, Gaggar, A, Gharwan, H and Lieber, A (2003). The interaction between the fiber knob domain and the cellular attachment receptor determines the intracellular trafficking route of adenoviruses. *J Virol* **77**: 3712–3723.
29. Ichida, S, Yuzawa, Y, Okada, H, Yoshioka, K and Matsuo, S (1994). Localization of the complement regulatory proteins in the normal human kidney. *Kidney Int* **46**: 89–96.
30. Maisner, A, Zimmer, G, Liszewski, MK, Lublin, DM, Atkinson, JP and Herrler, G (1997). Membrane cofactor protein (CD46) is a basolateral protein that is not endocytosed. Importance of the tetrapeptide FTSL at the carboxyl terminus. *J Biol Chem* **272**: 20793–20799.
31. Shayakhmetov, DM, Papayannopoulou, T, Stamatoyannopoulos, G and Lieber, A (2000). Efficient gene transfer into human $CD34^+$ cells by a retargeted adenovirus vector. *J Virol* **74**: 2567–2583.
32. Stone, D, Liu, Y, Li, ZY, Tuve, S, Strauss, R and Lieber, A (2007). Comparison of adenoviruses from species B, C, e, and f after intravenous delivery. *Mol Ther* **15**: 2146–2153.
33. Nanda, A, Lynch, DM, Goudsmit, J, Lemckert, AA, Ewald, BA, Sumida, SM *et al.* (2005). Immunogenicity of recombinant fiber-chimeric adenovirus serotype 35 vector-based vaccines in mice and rhesus monkeys. *J Virol* **79**: 14161–14168.
34. Lemckert, AA, Sumida, SM, Holterman, L, Vogels, R, Truitt, DM, Lynch, DM *et al.* (2005). Immunogenicity of heterologous prime-boost regimens involving recombinant adenovirus serotype 11 (Ad11) and Ad35 vaccine vectors in the presence of anti-Ad5 immunity. *J Virol* **79**: 9694–9701.
35. Nazir, SA and Metcalf, JP (2005). Innate immune response to adenovirus. *J Investig Med* **53**: 292–304.
36. Mizuguchi, H and Hayakawa, T (2002). Enhanced antitumor effect and reduced vector dissemination with fiber-modified adenovirus vectors expressing herpes simplex virus thymidine kinase. *Cancer Gene Ther* **9**: 236–242.
37. Okada, Y, Okada, N, Mizuguchi, H, Hayakawa, T, Mayumi, T and Mizuno, N (2003). An investigation of adverse effects caused by the injection of high-dose TNFα-expressing adenovirus vector into established murine melanoma. *Gene Ther* **10**: 700–705.
38. Mizuguchi, H and Kay, MA (1998). Efficient construction of a recombinant adenovirus vector by an improved *in vitro* ligation method. *Hum Gene Ther* **9**: 2577–2583.
39. Mizuguchi, H and Kay, MA (1999). A simple method for constructing E1- and E1/E4-deleted recombinant adenoviral vectors. *Hum Gene Ther* **10**: 2013–2017.
40. Sakurai, F, Kawabata, K, Yamaguchi, T, Hayakawa, T and Mizuguchi, H (2005). Optimization of adenovirus serotype 35 vectors for efficient transduction in human hematopoietic progenitors: comparison of promoter activities. *Gene Ther* **12**: 1424–1433.
41. Maizel, JV, Jr, White, DO and Scharff, MD (1968). The polypeptides of adenovirus. I. Evidence for multiple protein components in the virion and a comparison of types 2, 7A, and 12. *Virology* **36**: 115–125.
42. Nakamura, T, Sato, K and Hamada, H (2003). Reduction of natural adenovirus tropism to the liver by both ablation of fiber-coxsackievirus and adenovirus receptor interaction and use of replaceable short fiber. *J Virol* **77**: 2512–2521.
43. Sakurai, F, Nishioka, T, Saito, H, Baba, T, Okuda, A, Matsumoto, O *et al.* (2001). Interaction between DNA-cationic liposome complexes and erythrocytes is an important factor in systemic gene transfer via the intravenous route in mice: the role of the neutral helper lipid. *Gene Ther* **8**: 677–686.

Mutation Research 673 (2009) 9–20

Contents lists available at ScienceDirect

Mutation Research/Genetic Toxicology and Environmental Mutagenesis

journal homepage: www.elsevier.com/locate/gentox
Community address: www.elsevier.com/locate/mutres

Dose-dependent alterations in gene expression in mouse liver induced by diethylnitrosamine and ethylnitrosourea and determined by quantitative real-time PCR☆

Takashi Watanabe[a], Gotaro Tanaka[b], Shuichi Hamada[c], Chiaki Namiki[d], Takayoshi Suzuki[e], Madoka Nakajima[f], Chie Furihata[a,*]

[a] Functional Genomics Laboratory, School of Science and Engineering, Aoyama Gakuin University, Fuchinobe 5-10-1, Sagamihara, Kanagawa 229-0006, Japan
[b] Tokushima Research Center, Taiho Pharmaceutical Co. Ltd., Hiraishiebisuno 224-2, Kawauchichou, Tokushima, Tokushima 771-0194, Japan
[c] Genetic Toxicology Group, Toxicology Division II, Kashima Laboratory, Mitsubishi Chemical Safety Institute Ltd., Sunayama 14, Kamisu-shi, Ibaraki 314-0255, Japan
[d] Central Research Laboratory, SSP Co. Ltd., Nanpeidai 1143, Narita, Chiba 286-8511, Japan
[e] Division of Cellular & Gene Therapy Products, National Institute of Health Sciences, Kamiyoga 1-18-1 Setagaya-ku, Tokyo 158-8501, Japan
[f] Genetic Toxicology Group, Biosafety Research Center, Foods, Drugs, and Pesticides, Shioshinden 582-2, Fukude-cho, Iwata-gun, Shizuoka 437-1213, Japan

ARTICLE INFO

Article history:
Received 29 September 2008
Received in revised form 31 October 2008
Accepted 9 November 2008
Available online 21 November 2008

Keywords:
Genotoxic carcinogens
Dose-dependent alteration
Hierarchical clustering
k-means clustering
IPA

ABSTRACT

We examined the dose-dependency of gene expression changes for 51 genes in mouse liver treated with two *N*-nitroso genotoxic hepatocarcinogens, diethylnitrosamine (DEN) and ethylnitrosourea (ENU) by quantitative real-time PCR (qPCR). DEN (3, 9, 27 and 80 mg/kg bw) or ENU (6, 17, 50 and 150 mg/kg bw) was injected intraperitoneally into groups of five male 9-week-old B6C3F$_1$ mice and the livers were dissected after 4 h and 28 days. Total RNA from pooled livers was reverse-transcribed to cDNA and the amount of each gene was quantified by qPCR. Results were analyzed by hierarchical and *k*-means clustering and ingenuity pathway analysis (IPA). The most characteristic result was a similar dose-dependency of gene expression changes with DEN and ENU. Twenty-one genes exhibited a distinct dose-dependent increase in expression at 4 h for both carcinogens [*Bax*, *Btg2*, *Ccng1*, *Cdkn1a*, *Cyp4a10*, *Cyp21a1*, *Fos*, *Gadd45b*, *Gdf15*, *Hmox1*, *Hspb1*, *Isg20l1*, *Jun*, *Mbd1*, *Mdm2*, *Myc*, *Net1*, *Plk2*, *Ppp1r3c*, *Rcan1* and *Tubb2c*], although the increase in gene expression due to ENU was generally weaker than that due to DEN. Only *Gdf15* showed a dose-dependent increase in expression at 28 days for both carcinogens. The differences between DEN and ENU were in the expression of additional genes (7 for DEN and 8 for ENU). IPA extracted five gene networks: Network-1 included genes related to cancer and cell cycle arrest and associated with *Bax*, *Btg2*, *Ccng1*, *Cdkn1a*, *Gadd45b*, *Gdf15*, *Hspb1*, *Mdm2* and *Plk2* and Network-2 was related to DNA replication, recombination, repair and cell death and associated with *Cyp21a1*, *Gdf15*, *Ppp1r3c*, *Rcan1* and *Tubb2c*. The present results show a distinct dose-dependency of gene expression changes induced by DEN and ENU. These changes were associated with cancer, cell cycle arrest, DNA replication, recombination, repair and cell death and were seen not only at 4 h but also, for some, at 28 days after administration.

1. Introduction

Diethylnitrosamine (DEN) and ethylnitrosourea (ENU) are potent genotoxic *N*-nitroso carcinogens that induce hepatocellular carcinomas in mouse liver [1,2]. It has been reported that after its metabolic biotransformation, DEN produces the promutagenic adducts O^6-ethylguanine (O^6-EtG) and O^4- and O^2-ethylthymine and that O^4-ethylthymine may be responsible for the initiation of hepatocellular carcinomas in rats [3]. ENU, which is a direct-ethylating agent, forms several major adducts upon reaction with DNA, of which O^6-EtG, O^4- and O^2-ethylthymine and N^3-ethylthymine have been implicated in mutagenic lesions [4]. Suzuki et al. have reported that mutagenic activity by DEN and ENU was clearly detected with the *lacZ* mutation assay in mouse liver at 7 days [5]. Mientjes et al. have reported that the O^6-EtG levels increased as early as 1.5 h after treatment, whereas at 3 days more than 90% of the lesions had been removed from the DNA in the livers of DEN- and ENU-treated mice, based on *lacZ* transgenic mice [6]. After this period, however, with the bulk of O^6-EtG removed, the induction of *lacZ* mutations was observed at 3 days and continued to increase for some weeks.

☆ This work was a JEMS/MMS/Toxicogenomics group collaborative study.

* Corresponding author at: Department of Chemistry and Biological Science, School of Science and Engineering, Aoyama Gakuin University, 5-10-1 Fuchinobe, Sagamihara, Kanagawa 229-8558, Japan. Tel.: +42 759 6233; fax: +42 759 6511.
E-mail address: chiefurihata@gmail.com (C. Furihata).

1383-5718/$ – see front matter © 2008 Elsevier B.V. All rights reserved.
doi:10.1016/j.mrgentox.2008.11.004

Previously, Waring et al. showed by DNA microarray that a number of genes are up-regulated and down-regulated in rat liver, with rats dosed daily with DEN for 3 days and euthanized on the 4th day [7]. Genes up-regulated by DEN included genes related to growth arrest and DNA damage, such as *Bax*, *Ccnd1*, *Ccng1*, *Cdkn1a/p21*, *Gadd45* and *Jun*. However, no studies have focused on either the DNA damaging time of 4 h or the mutation fixing time of 28 days in DEN-treated mouse or rat liver. Although it has been reported that ENU induced expression of *Bax*, *Crp*, *Cyp2a*, *Gstm2*, *Icam1*, *Mig*, and *Mt2* mRNA in mouse liver, little is known about differential gene expression in ENU-exposed rodent liver [8].

Quantitative real-time PCR (qPCR) is an alternative technology for toxicogenomics [9]. qPCR is a highly regarded and reliable quantitative method but analysis of a large number of genes may be lengthy. It is impractical to examine a great number of genes with qPCR. Therefore, we selected 51 candidate genes (Table 1) based on our previous results using the Affymetrix GeneChip Mu74AV2 and original DNA microarray to determined the effects of DEN, dimethylnitrosamine, dipropylnitrosamine, ENU, *o*-aminoazotoluene, 7,12-dimethylbenz[*a*]anthracene, dibenzo[*a*,*l*]pyrene, phenobarbital and ethanol exposure in mouse liver for 4 and 20 h and 14 and 28 days in our JEMS/MMS/Toxicogenomics group collaborative study; results were reported in part [10]. We examined gene expression changes at an early time after administration, as we were interested in whether toxicogenomics was useful for carcinogen screening. In the previous study, using a single dose for each chemical, gene expression changes in number and degree were observed to peak at 4 h after administration. It is known that genotoxic *N*-nitroso carcinogens induce DNA damage and repair in a matter of a few hours after their administration; DNA adducts [6], DNA strand-breaks [11], unscheduled DNA synthesis [12] and other lesions have been reported. It is also known that mutations are observed in transgenic mouse liver 28 days after genotoxic *N*-nitroso carcinogen administration [5,6]. However, related gene expression changes at these time points have not yet been fully elucidated.

Table 1
Fifty-one genes examined in the present study.

No.	Symbol	Gene name	Accession number
1	*Bax*	Bcl2-associated X protein	NM_007527
2	*Bcl2*	B-cell leukemia/lymphoma 2	NM_009741
3	*Btg2*	B-cell translocation gene 2, anti-proliferative	NM_007570
4	*Casp1*	IL-1B converting enzyme; interleukin 1 beta-converting enzyme	NM_009807
5	*Ccnf*	Cyclin F	NM_007634
6	*Ccng1*	Cyclin G1	NM_009831
7	*Ccng2*	Cyclin G2	NM_007635
8	*Cdkn1a (p21)*	Cyclin-dependent kinase inhibitor 1A (P21)	NM_007669
9	*Cyp1a1*	Cytochrome P450, family 1, subfamily a, polypeptide 1	NM_009992
10	*Cyp1a2*	Cytochrome P450, family 1, subfamily a, polypeptide 2	NM_009993
11	*Cyp4a10*	Cytochrome P450, family 4, subfamily a, polypeptide 10	NM_010011
12	*Cyp21a1*	Cytochrome P450, family 21, subfamily a, polypeptide 1	NM_009995
13	*Dpyd*	Dihydropyrimidine dehydrogenase	NM_170778
14	*Egfr*	Epidermal growth factor receptor	NM_207655
15	*Ephx1*	Epoxide hydrolase 1, microsomal	NM_010145
16	*Fabp5*	Fatty acid binding protein 5, epidermal	NM_010634
17	*Fos*	FBJ osteosarcoma oncogene	NM_010234
18	*Gadd45b*	Growth arrest and DNA-damage-inducible 45 beta	NM_008655
19	*Gadd45g*	Growth arrest and DNA-damage-inducible 45 gamma	NM_011817
20	*Gapdh*	Glyceraldehyde-3-phosphate dehydrogenase	NM_008084
21	*Gdf15*	Growth differentiation factor 15	NM_011819
22	*Glul*	Glutamate-ammonia ligase (glutamine synthetase)	NM_008131
23	*Gstk1*	Glutathione S-transferase kappa 1	NM_029555
24	*Gyk*	Glycerol kinase	NM_212444
25	*Hist1h1c*	H1 histone family, member 2	NM_015786
26	*Hspa1b (Hsp70)*	Heat shock protein 1B	NM_010478
27	*Hspb1*	Heat shock protein 1	NM_013560
28	*Hspb2 (Hsp27)*	Heat shock protein 2	NM_024441
29	*Hmox1*	Heme oxygenase (decycling) 1	NM_010442
30	*Hprt1*	Hypoxanthine guanine phosphoribosyl transferase 1	NM_013556
31	*Igfbp1*	Insulin-like growth factor binding protein 1	NM_008341
32	*Isg20l1*	Interferon stimulated exonuclease gene 20-like 1	NM_026531
33	*Jun*	Jun oncogene	NM_010591
34	*Kras*	v-Ki-ras2 Kirsten rat sarcoma viral oncogene homolog	NM_021284
35	*Lig3*	Ligase III, DNA, ATP-dependent	NM_010716
36	*Lrp1*	Low density lipoprotein receptor-related protein 1	NM_008512
37	*Mbd1*	Methyl-CpG binding domain protein 1	NM_013594
38	*Mdm2*	Transformed mouse 3T3 cell double minute 2	NM_010786
39	*Myc*	Myelocytomatosis oncogene	NM_010849
40	*Net1*	Neuroepithelial cell transforming gene 1	NM_019671
41	*Pdgfb*	Platelet-derived growth factor, B polypeptide	NM_011057
42	*Plk2*	Polo-like kinase 2; serum-inducible kinase	NM_152804
43	*Pml*	Promyelocytic leukemia	NM_008884
44	*Pmm1*	Phosphomannomutase 1	NM_013872
45	*Ppp1r3c*	Protein phosphatase 1, regulatory (inhibitor) subunit 3C	NM_016854
46	*Rad52*	RAD52 homolog (S. cerevisiae)	NM_011236
47	*Rcan1(Dscr1)*	Regulator of calcineurin 1	NM_019466
48	*Trp53*	Transformation related protein 53	NM_011640
49	*Tubb2c*	Tubulin, beta 2c	NM_146116
50	*Ube2e1 (UbcM3)*	Ubiquitin-conjugating enzyme E2E 1, UBC4/5 homolog (yeast)	NM_009455
51	*Ung*	Uracil-DNA glycosylase	NM_011677